REVIEW

Chitosan-based nanocomposites for medical applications

Selvakumar Murugesan[1,2] | **Thomas Scheibel**[1,3]

[1]Lehrstuhl Biomaterialien, Universität Bayreuth, Bayreuth, Germany

[2]Department of Metallurgical and Materials Engineering, National Institute of Technology Karnataka, Mangalore, India

[3]Bayreuther Zentrum für Kolloide und Grenzflächen (BZKG), Bayreuther Zentrum für Molekulare Biowissenschaften (BZMB), Bayreuther Materialzentrum (BayMAT), Bayerisches Polymerinstitut (BPI), University Bayreuth, Bayreuth, Germany

Correspondence

Thomas Scheibel, Lehrstuhl Biomaterialien, Universität Bayreuth, Prof.-Rüdiger-Bormann.Str. 1, 95447 Bayreuth, Germany.
Email: thomas.scheibel@bm.uni-bayreuth.de

Abstract

Chitosan as a biobased polymer is gaining increasing attention due to its extraordinary physico-chemical characteristics and properties. While a primary use of chitosan has been in horticultural and agricultural applications for plant defense and to increase crop yield, recent research reports display various new utilizations in the field of advanced biomedical devices, targeted drug delivery, and as bioimaging sensors. Chitosan possesses multiple characteristics such as antimicrobial properties, stimuli-responsiveness, tunable mechanical strength, biocompatibility, biodegradability, and water-solubility. Further, chitosan can be processed into nanoparticles, nano-vehicles, nanocapsules, scaffolds, fiber meshes, and 3D printed scaffolds for a variety of applications. In recent times, nanoparticles incorporated in chitosan matrices have been identified to show superior biological activity, as cells tend to proliferate/differentiate faster when they interact with nanocomposites rather than bulk or micron size substrates/scaffolds. The present article intents to cover chitosan-based nanocomposites used for regenerative medicine, wound dressings, drug delivery, and biosensing applications.

KEYWORDS

chitosan, nanocomposites, nanoparticles, regenerative medicines and drug delivery

1 | INTRODUCTION

Nature-derived materials provide plenty of features to outcompete man-made synthetic materials in various applications in industries ranging from cosmetics to aerospace.[1] Concerning biomedical applications, natural materials are often superior to synthetic materials due to their multiple characteristics and properties.[2–6] Among various natural polymers, for biomedical applications water-soluble polymers with salient biological characteristics are preferred over polymers dissolving only in organic/inorganic solvents.[7] Chitosan is a polysaccharide and a chemical derivative of chitin. Henni Braconnot, a French professor, was the first one who extracted chitin from mushrooms in 1811s.[8] Later chitin was isolated from many invertebrate animals such as mollusca, crabs, prawns shrimps, crayfishes, and lobsters by various scientists. Among all, shells of crabs and shrimps are the most abundant sources for chitin. Chitins are polymers based on a disaccharide of 2-acetamido-2-deoxy-β-D-glucose linked by a β (1 → 4) bond. In the 19th century, chitosan was unveiled upon deacetylation of chitin with abundant acetyl glucosamine units.[9] As a result, chitosan is a heteropolymer showing both glucosamine as well as acetyl glucosamine groups since the deacetylation is incomplete.[10] The presence of NH_2 groups enables tailoring of the characteristics of this polymer since they allow copolymerization using acrylic, styrene, urethane, and vinyl ester-based monomers to acquire supplementary properties.[11–14] The chemical structure of chitin and chitosan is shown in Figure 1. Chitosan

FIGURE 1 Top panel shows the chemical structure of chitin (*N*-acetylglucosamine) and chitosan, a deacetylated chitin (*N*-acetyl-D-glucosamine). Bottom panel shows various important chemical modification steps of chitosan: (A) methylation, (B) thiolation, (C) azylation, (D) co-polymerization with acrylic monomer, (E) *N*-succinylation (Reproduced with permission from Jayakumar et al.,[15] Shukla et al.,[16] and Ravi Kumar et al.[17])
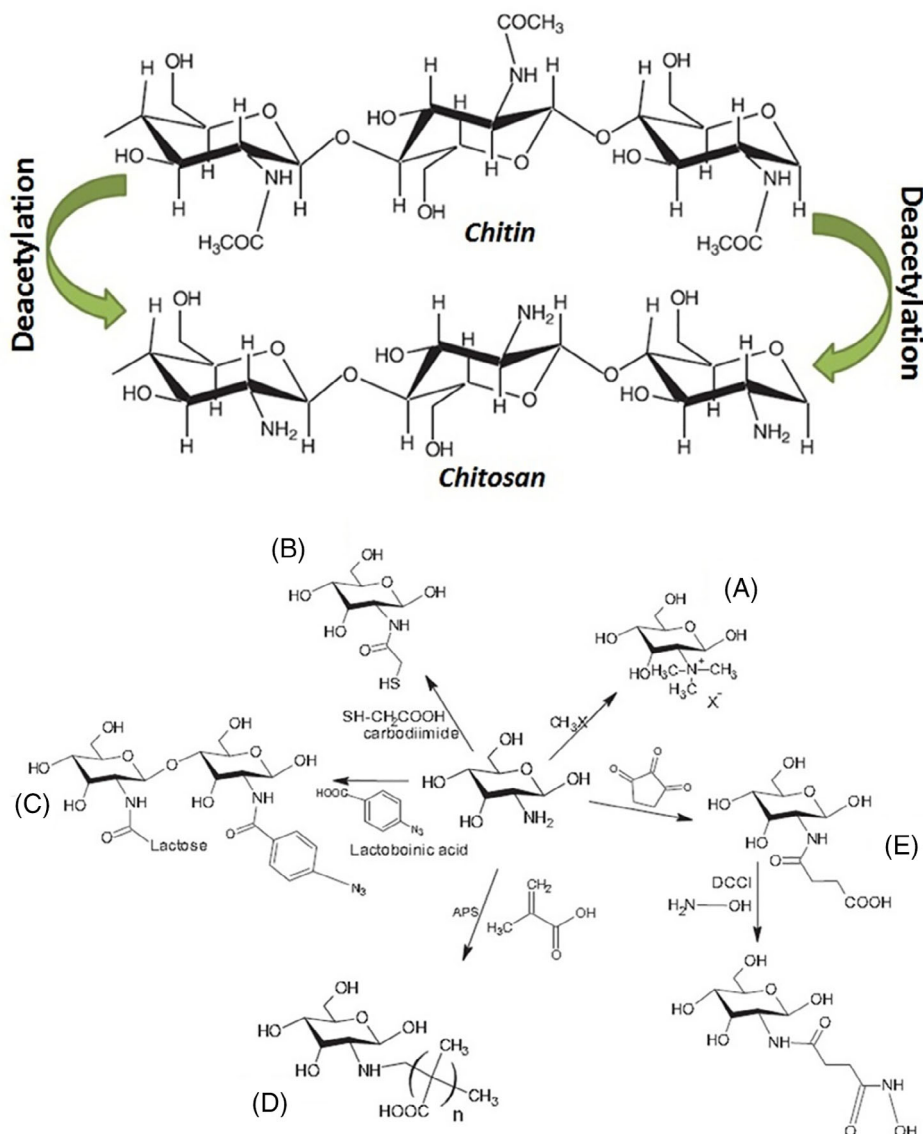
polymers are easily dissolvable at acidic conditions, unlike chitin.[18] The % content of glucosamine and acetyl glucosamine moieties dictates the properties of chitosan including physico-chemical and biological characteristics. Chitosan is biodegradable, analgesic, antibacterial, antifungal, and hemostatic. Furthermore, the degree of deacetylation (DD) influences the mucoadhesive characteristics of chitosan.[19] The number of products available manifests the dominance of chitosan since 1995 compared to other biopolymers including poly(L-lactic acid), collagen, gelatin, or silk protein.[20] Among various biopolymers, chitosan is preferred for various biomedical products due to its abundant biological properties like antimicrobial activity, hemostasis, macrophage immune responses, capability to stimulate pro- and anti-inflammatory cytokines, lipids, various growth factors and chemokines, polyelectrolyte complex formation, mucoadhesive strength, and higher friability of tablets.[21] Such multifunctional features

have not yet been reported for other biopolymers apart from chitosan. Therefore, chitosan made an entry to various medical applications including tissue regeneration, drug delivery, biosensors, and wound dressings.

Various chemical routes have been used to modify chitosan such as nitration, alkylation, sulphonation, phosphorylation, xanthation, schiff's base formation, acylation, hydroxylation, and graft copolymerization.[12] Figure 1 displays some of the important steps involved in the chemical modification of chitosan.

Recently, the properties of nanoparticles have made them interesting for fabricating nanocomposites especially for biomedical applications such as targeted delivery (drug and gene), bioimaging, and regeneration of tissue like skins and bone.[22] Cells cultured on chitosan-based nanocomposites proliferate fast, and such scaffolds promote cell differentiation without any growth factors, which is very useful for tissue regeneration.[23] For tissue

engineering, developing a substrate or biomaterial imitating the cellular environment is one important key factor.[24] A perfect biomaterial provides mechanical support as well as simulates the cells to differentiate into specific cell types. Nanocomposite substrates offer additional properties such as antimicrobial or antifungal ones to avoid tissue damage from infection/inflammation, which is one of the key factors hindering tissue regeneration upon implantation of new tissue.[25] One advantage of chitosan is that its surface adsorbs proteins rapidly.[26] Several articles reviewed the biomedical applications of chitosan-based nanocomposites in suspensions like nanogels and micelles.[27–33] This article reports on chitosan-based nanocomposite scaffolds with a focus on tissue engineering.

2 | CHITOSAN-BASED NANOCOMPOSITE SCAFFOLDS FOR TISSUE ENGINEERING

Many features such as cytotoxicity, mechanical properties as well as healing efficiencies have to be considered while fabricating a scaffold/substrate for tissue regeneration. Various existing methodologies have been adapted for processing of chitosan-based nanocomposites into films,[34] fiber-meshes,[35] hydrogels,[36–40] and 3D printed constructs[41] to mimic the 3D environment of tissues. Processing into a freestanding thin film is the easiest choice and affordable route to evaluate the physico-mechanical properties and biocompatibility of the designed nanocomposites.[42–44] Chitosan nanocomposite thin films can be fabricated using solution casting, melt mixing, and in-situ nanoparticle synthesis approaches. Solution casting is usually carried out using water, cell culture medium, and sometimes organic solvents. Additionally, ultrasonication is often used to disperse the nanofillers effectively.[45] Twin-screw extruders, injection molding, and blow molding have been used for melt mixing approaches in order to fabricate chitosan nanocomposites.[46] In an in-situ method, chitosan has been used as a surfactant for the synthesis of nanoparticles. These approaches do not need a large quantity of materials, and any kind of shape and size can be manufactured.[47] The surface characteristics of freestanding films can be fine-tuned by different post-treatment techniques. Owing to its outstanding mechanical and biological properties, chitosan nanocomposite films have already been used in various biomedical applications including wound dressing patches,[48–51] drug delivery,[52,53] implant coatings,[54–56] and as scaffolds.[57,58] Various nanoparticles such as nanoclay,[59] graphene,[60] silver,[61] cellulose whisker,[62] and titania[63] have been used for the preparation of chitosan nanocomposites films for such applications.

Beyond films, chitosan-based hydrogels are fascinating biomaterials, as they possess a high amount of water, which makes them well compatible with most of the native tissues.[7,38,40,54] Gels comprise up to 10% solid-phase in a total volume of the gel (the rest is water or liquid phase). This 10% solid phase warrant the consistency of the gel. Most importantly, hydrogels are mostly very soft in nature and often self-recoverable in shape, which will be useful during, for example, implantation. Besides that, mechanical responses of hydrogels are likely to imitate that of native soft tissues, which will make it easier to assure the functional characteristics of the tissue to be repaired.[16,36,37,39] This is one major reason why hydrogels are used as scaffolds in biomedical applications. Nanoparticle incorporation into a chitosan matrix enhances mechanical strength, shape recovery, and stimuli-response of chitosan-based hydrogels.

Sponges are a scaffold morphology with plenty of micron sized open pores. The open pores can intake a large number of fluids beneficial for cell growth as well as proliferation.[64,65] Chitosan-based nanosponges can be fabricated by many techniques such as freeze-drying (lyophilisation) and by introducing foaming agents during melt mixing of chitosan and nanoparticles.[65,66] Among them, a simple and efficient process is lyophilisation, which starts with freezing a solution of chitosan with or without additives followed by evaporation of the solvent under reduced pressure.[67,68]

At present, there are numerous techniques available to fabricate a chitosan-based membrane or scaffold for tissue engineering such as particle salt leaching,[69,70] electrospinning,[71,72] stereolithography,[73,74] gas foaming,[75,76] freeze-drying,[57,67,75] and 3D bioprinting.[77–80] Electrospinning is a simple, straightforward, and cost-effective technique for producing nanofibers. In a typical electrospinning set-up, high voltage is applied from a polymeric solution to draw fibers toward a grounded collector.[72] The spinning characteristics and efficiencies can be improved by incorporating nanoparticles into chitosan solutions as this can change the solution properties like conductivity and viscosity, which inherently improves the spinnability of the polymer dope.[29,71] 3D bioprinting has exciting prospects since it shows many advanced features like the capability of printing tissue-analog structures, or constructing 3D scaffolds with more than two types of cells within a suitable matrix, which can bring extraordinary functional characteristics and provide faster tissue regeneration.[77,80] The main concept of producing 3D tissue constructs using bioprinting is based on additive manufacturing approaches to construct a complex structure, which mimics the parent tissue via a layer-by-layer method.[79] Depending on the type of bioprinter, the choice of materials can be varied. The design

protocol for printable materials plays a key role in printing characteristics. The water-soluble nature of chitosan biopolymer made it easy to assemble hydrogels at certain pH values and temperatures, which showed properties useful for 3D bioprinting.[78] So far, very few researchers have explored chitosan-based nanocomposite bioinks for 3D printing but the number of reports is raising. In the subsequent sections, various aspects of chitosan nanocomposites for tissue engineering applications are discussed in detail.

2.1 | Chitosan nanocomposites for bone engineering

At present, a large number of patients requires organ transplantation including bone, heart, liver, kidney, and so forth.[81] Tendons, ligaments, skin, heart valves, blood vessels, and bones are the most commonly transplanted organs in the world.[82] Taking bone as one example, transplanting bone in patients above 50 years old is a significant clinical challenge faced by orthopedics. Even though bone has a certain healing ability, large defects caused by age, traffic accidents, and bone tumor resection prevent good bone regeneration. Therefore, novel approaches for repairing bone defects have to be developed. Bone is composed in its majority of pentacalcium phosphates, collagen, several other proteins, as well as cells such as osteoblasts, osteocytes, and osteoclasts.[83] The major function of bone is to provide a skeleton with load-bearing capacity and to protect the internal organs. Bone experiences a constant cycle of resorption and remodeling.[84,85] Although, our body can constantly repair bone tissue defects, larger defects need medical treatment. Traditionally, autografts, allografts, and xenograft are used in clinical practice to restore/repair damaged tissues.[86] Among these, autografts are considered the gold standard, for which cells from the injured person are harvested to repair or restore the damaged tissue.[87] However, autografts have some limitations such as low availability, discomfort, scar formation, and donor site morbidity. In allografts, cells from other persons than the patient but of the same species and in xenografts, cells from a different species such as pigs are used to repair or restore tissues. These grafting methods are risky because of possible tissue rejections, mismatching, and disease transmission.[88] The basis for choosing a fitting biomaterial for bone tissue engineering is a thorough understanding of bone anatomy and the healing process. Bone healing is a complex process, and the recovery and success rate vary from person to person. Recent developments in bone tissue engineering use three-dimensional (3D) processing technologies, which provide mechanical,

cellular, and molecular enviroments to repair, retain, or recover injured bone tissue.

In the context of choosing fitting biomaterials, chitosan nanocomposites with nanofillers like hydroxyapatite,[75,89,90] bioactive glass,[23,91] zeolite,[92] copper nanoparticles,[93] and carbon filler,[27,43,93] and so forth are extensively used for bone tissue engineering applications and they are applied as thin films, fiber-meshes, scaffolds, and hydrogels.[94] Chitosan nanocomposites of choice for bone engineering applications are summarized in Table 1.

Cao et al.[140] prepared 2-N,6-O-sulfated chitosan/calcium phosphate nanocomposite hydrogels loaded with bone morphogenetic protein 2 (BMP-2) for the regeneration of critical-size bone defect in rabbits showing enhanced vascularisation. An in vitro alkaline phosphatase (ALP) assay confirmed the activity of released BMP-2 from the developed hybrid gel after 3 and 7 days of delivery. The robust angiogenesis of the prepared hybrid gel was confirmed by both in vitro as well as in vivo tests in the critical-sized defect (18 mm radius) of the rabbit. Blood vessel formation was thoroughly investigated using synchrotron radiation-based micro-computed tomography imaging, three dimensional micro-computed tomographic imaging, histological analysis, immunohistochemistry, and biomechanical measurements. Figure 2 shows micro-computed tomography images used for quantitative analysis of new bone (NB) formation followed by the amount of blood vessel formation for various samples. μCT results revealed that hybrid gels displayed the best performance concerning vascularisation as well as volume of NB formation. The results implied that BMP 2 alone is not able to augment the blood vessel formation in the defect. The BMP-2/SNP/G hybrid facilitated formation of more blood vessels as well as larger volumes of NBs by faster biomineralization. The improved angiogenesis was confirmed by studying the relative gene expression of endothelial markers such as endothelial cell differentiation (CD31) and endothelial cell–derived von Willebrand Factor (vWF) assayed using real-time quantitative reverse transcription polymerase chain reaction (qRT-PCR) at day 7. Histopathology using hematoxylin and eosin (H&E) staining (Figure 3) revealed the formation of blood cells (BC) and macrophages (yellow line) at 2 weeks after implantation. At four-week post-implantation, the development of chondrocytes (CC) was noticed. After 8 weeks, a larger volume of NB was observed in case of hybrid gels. More BC, macrophages, OC, and NB were found in that experimental group compared to the other samples.

There are many reports on mechanical properties of chitosan-ceramic nanocomposites and their comparison to various human bone tissues.[141–145] Xiao et al.[142] studied the mechanical properties of hydroxyapatite

TABLE 1 Chitosan nanocomposite substrates for bone engineering

Nanocomposites additives	Fabrication method and chitosan details (if available)	Features in comparison to pristine chitosan materials	Cell line and cytotoxicity in comparison to pristine chitosan materials evaluation (if available)
Chitosan Films			
Erbium doped fluorescent hydroxyapatite nanoparticles[95]	Solution casting/M_w of 100,000–300,000 g/mol and 85% DDA	• Antimicrobial activity and hydrophilicity • Biocompatibility, robust cell proliferation, tuned biodegradability, and biomineralization • Fluorescent nanoparticles helped for cell localisation	Human lung fibroblasts (WI-38), cell viability was above 80% after 24 h of culture.
Tobermorite type nanoclay[96]	Solvent casting/low-molecular-weight	• Bioactivity and biodegradation • Cell compatibility	MG63 human osteosarcoma cells, cell viability enhanced up to 30%.
Nano bioglass embedded in chitosan–polycaprolactone bilayered films[97]	Solution casting	• Mechanical properties, bioactivity, and biodegradation • Cell viability was higher for monolayer films	MG-63 osteoblast-like cells, cell viability was 98% for monolayer films
Bioactive glass nanoparticles[98]	Solution casting/M_w of 190,000–310,000 g/mol, 75%–85% DDA, and a viscosity of 200–800 cps	• Cell metabolic activity, proliferation, calcium deposition, DNA content, and biomineralization • Mechanical properties significantly deteriorated	Human periodontal ligament cells and Human bone marrow stromal cells
Zirconium oxide nanoparticles[99]	Solution casting/M_w of 230,000 g/mol, and 86% DDA	• Adequate tensile strengths, excellent microbial protection against gram-negative and gram-positive bacterial strains • Excellent biocompatibility and >5% hemolysis	Human osteoblastic MG-63 cells, cell viability up to 55%
Copper nanoparticles[100]	Solution casting/low-molecular-weight chitosan, which has 85% DDA	• Remarkable anticancer effect due to a higher amount of mitochondrial reactive oxygen species (ROS and enhanced caspase activity)	Human osteosarcoma cell line MG-63, 85% cells were dead upon incorporation of copper nanoparticles
Hydroxyapatite and silica[101]	Solution casting/85% DDA	• good apatite layer formation, cell viability, as well as rate of cell proliferation	Rat osteoblast-like UMR-106 cells
Zirconia (ZrO$_2$) nanoparticles reinforced chitosan and poly(vinyl alcohol), PVA blends[102]	Solution casting/M_w of 230,000 g/mol with 86% DDA	• Excellent mechanical properties such as tensile strength, % elongation, modulus, % cell viabilities and rate of cell proliferation	Human osteoblastic MG-63 cells, cell viability was increased up to 15%
Hydroxyapatite[103]	Solution casting/chitosan had above 95% DDA	• Excellent osteodifferentiation characteristics like alkaline phosphatase (ALP) content increased by 377%, collagen I increased by 479, and osteopontin increased by 597%	Mesenchymal stem cells (MSCs), cell viability increased by 52%
Nano-hydroxyapatite and silver[104]	Solution blending/low-molecular-weight and 75%–85% DDA	• Enhanced mechanical properties, antimicrobial activities, rate of biodegradation, cell penetration, adhesion and spreading efficiency.	Rat osteoprogenitor cells and human osteosarcoma cells

TABLE 1 (Continued)

Nanocomposites additives	Fabrication method and chitosan details (if available)	Features in comparison to pristine chitosan materials	Cell line and cytotoxicity in comparison to pristine chitosan materials evaluation (if available)
Euryale ferox modified hydroxyapatite nanoparticles[105]	Solution casting/85% DDA	• Enhanced biomineralization, antibacterial activity, cell viability, differentiate into osteogenic lineage and biodegradation.	Human osteoblasts like MG-63 cells, cell viability was above 95%
Chemically exfoliated GO sheets[106]	Solution casting/M_w of 90,000–150,000 g/mol and 80% DDA	• Enhanced tensile strength and elastic modulus, antibacterial activity (>77%), high cell viability. • Above 5 wt% GO reinforcement decelerated the cell proliferation	Human mesenchymal stem cells, cells viability was up to 90%
Naturally derived hydroxyapatite (*Thunnus obesus* bone) reinforced MWCNT-grafted-chitosan[107]	Solution casting/M_w of 500,000 g/mol with 70%–90% DDA	• Decreased % water uptake, retention ability and bio degradation for the nanocomposites. • Thermal stability and % cell viability were significantly increased	Human osteosarcoma cell line (MG-63 cells), cell viability increased by 2-fold
Carboxylic functionalised MWCNT embedded in chitosan/hydroxyapatite blend[108]	In situ approach followed by solution casting/M_w of 1,000,000 g/mol with 95% DDA	• Superior mechanical strength observed for the nanocompsoites blend. • Cell adhesion found to be almost similar and cell proliferation was slightly higher	MC3T3-E1 cells, cell proliferation increased by $2\frac{1}{4}$-fold
Chitosan scaffolds (sponges, hydrogels, etc.)			
Silicon dioxide and zirconia nano particles[109]	Freeze-drying method/low-molecular-weight with 75%–85% DDA	• Improved % deswelling and biodegradation rate, protein adsorption, and rapid biomineralization capabilities	Osteoprogenitor cells. Nanocomposites scaffold showed non-toxicity at lower concentrations of silicon dioxide and zirconia nano particles encapsulation.
Hydroxyapatite[110]	Solution method/M_w of 310,000 g/mol with 90% DDA	• In vitro cell uptake and proliferation was superior • In vivo study confirmed the new bone formation, trabecular thickness and bone remodeling	Preosteoblasts (MC3T3-E1)
Nano silver and hydroxyapatite particles[104]	Freeze-drying method/low-molecular-weight, which has 75%–85% DDA	• Improved antibacterial activity against both gram-positive and gram-negative bacterial strains. • No toxicology effect and high rate of biodegradation	Rat osteoprogenitor cells and human osteosarcoma cell line
In situ developed nano hydroxyapatite[111]	Co-precipitation technique followed by freeze drying method/93.5% DDA	• Enhanced biocompatibility	Clonal preosteoblastic cell line MC 3 T3-E1 cells. Cell viability increased up to 6-fold after 7 days of culture.
Nanocrystalline calcium phosphate[112]	Solution approach/92.3% DDA	• Improved mechanical properties, protein adsorption (fibronection), and cell adhesion, proliferation.	Human Embryonic Palatal Mesenchymal cells (HEPM), cell viability was above 65%.
Genipin crosslinked chitosan nano β-tricalcium phosphate[113]	Freeze-gel approach/85%DDA	• Adequate compressive strength, improved metabolic activity, higher wettability, great extent of mineralization	Human mesenchymal stem cells (hMSCs). Cell viability increased up to 2-fold after 5 days of culture.

(Continues)

TABLE 1 (Continued)

Nanocomposites additives	Fabrication method and chitosan details (if available)	Features in comparison to pristine chitosan materials	Cell line and cytotoxicity in comparison to pristine chitosan materials evaluation (if available)
Dual nanofillers of bioactive glass (BG) and CNT[114]	Salt-leaching approach/medium-molecular-weight with viscosity of 200-800 cP	• Enhanced compression strength, biodegradability, wettability, mineral deposition and cell compatibility	MG63 osteoblast cell line
Dual nanoparticles of hydroxyapatite and β-tricalcium phosphate (TCP) derived from waste mussel shells[115]	Freeze-drying method/chitosan derived from waste arrow squid pen (*Nototodarus sloanii*) had 75% DDA	• Enriched biodegradability of 90% after 28 days, cell viability, proliferation, and biomineralization	Human osteoblast-like cells (Saos-2) and mouse fibroblastic-like cells (L929). Cell viability increased by 2-fold for L929 and 5-fold for Saos-2
Bioglass[116]	Needle punching process	• Exhibited higher porosity of about 86% without affecting its mechanical stability. • Improved cell adhesion and proliferation	Human bone marrow stromal cells (hBMSCs), cell viability increased by 4-fold after 7 days of culture.
Nano-hydroxyapatite[117]	Freeze-drying method/80% DDA	• In vivo and 3D-μCT results showed ectopic osteogenesis, De novo bone, biodegradation and collagen formation were found to be greater	Rat bone marrow mesenchymal stem cell
Gadolinium phosphate nanoparticles[118]	Freeze-drying method	• The releasing spare amount of gadolinium ions (Gd^{3+}) helped to enhance cell viability or proliferation differentiation of stem cells toward osteogenic lineages such as improved ALP activity, Runx-2, osteocalcin secretion and Col-I expressions • In vivo results showed new bone formation, with dense collagen fibers in rat calvarial defect	Primary rat bone marrow mesenchymal stem cells (BMSCs), cell viability increased by 3-fold
$SrFe_{12}O_{19}$ based magnetic nanoparticles decorated-mesoporous bioglass[119]	Freeze-drying method	• Nanocomposites showed prominent expression levels of osteogenic lineages including osteocalcin, COL1, Runx2 and ALP activity, which enhance the bone regeneration • Exceptional antitumor effectiveness against osteosarcoma via the hyperthermia (NIR) ablation	Human bone marrow mesenchymal stem cells (hBMSCs)
Nano-hydroxyapatite[120]	Freeze-drying method/91.2% DDA	• Excellent regeneration ability of critical-sized calvarial bone defect (in vivo) • New bone formation and neovascularisation were also observed for the nanocomposite implants	Only in vivo assessment
2-*N*, 6-*O*-sulfated chitosan/ bone morphogenetic protein-2[121]	Hydrogels prepared by complex coacervation method and photopolymerisation. The chemically modified 2-*N*, 6-*O*-sulfated chitosan was obtained by the metal-complex tris (2,2′-bipyridyl) dichlororuthenium (II) hexahydrate ([RuII(bpy)₃]²⁺) and sodium persulphate	• Nanocomposite hydrogels improved bioactivity, induced ectopic bone formation, larger amount of new bone formation and induced reunion of the bone marrow cavity	Human mesenchymal stem cells (hMSCs) and Human umbilical vein endothelial cells (HUVECs). Cell proliferation was enhanced up to 180% after 7 days of culture.

TABLE 1 (Continued)

Nanocomposites additives	Fabrication method and chitosan details (if available)	Features in comparison to pristine chitosan materials	Cell line and cytotoxicity in comparison to pristine chitosan materials evaluation (if available)
Injectable hydrogels made of chitosan/β-glycerophosphate (CS/GP) reinforced with hydroxyapatite nanoparticles[122]	Solution blending method	• Nanocomposite hydrogels enhanced % cell viability, rate of cell proliferation and osteoblastic differentiation of MSCs	Mesenchymal stem cells. Cell viability increased up to 5-fold after 7 days of culture.
Injectable hydrogels made of nano-hydroxyapatite (n-HA) reinforced chitosan/ hyaluronic acid (HyA) blends[123]	Solution approach/glycol modified chitosan had a degree of polymerization of above 400	• Decreased % porosity and swelling ratio • Enhanced biodegradation rate via enzymatic hydrolysis, cell viability and proliferation	MC-3 T3-E1 cells, cell viability enhanced up to 90%
Chitosan blend scaffolds			
Hydroxyapatite reinforced blends of chitosan/gelatin/ alginate[124]	Foaming method by bead form/M_w of 100,000–300,000 g/mol	• Composite scaffolds displayed porosity of 82%, and excellent hydrophilicity, biodegradability. • Better cell attachment and proliferation as well as differentiability into osteogenic lineage	Osteoblast cells. Cell viability increased up to 1¼-fold.
Nano needular TiO_2 incorporated chitin-chitosan blends[125]	Lyophilization technique/M_w of 100,000–150,000 with 85% DDA	• Nanocomposite scaffold showed controlled swelling and degradation rate and excellent biomineralization • Improved cell uptake, adhesion and proliferation with the various types of cells	Osteoblast-like cells (MG-63), fibroblast cells (L929), and human mesenchymal stem cells (hMSCs). All cell lines showed improved cell attachment on nanocomposites scaffolds.
Nano-hydroxyapatite incorporated into the blends of chitosan and carboxymethyl cellulose[126]	Freeze-drying method/two types of chitosan used average M_v of 250,000 g/mol with 80% DDA and carboxymethyl cellulose - Na degree of substitution around 0.7 with M_v of 420,000,000 g/mol	• Nanocomposite scaffolds displayed 77.8% porosity, enhanced bioactivity, biomineralization and adequate compressive strength of 3.54 MPa	-
Microspheres from collagen/ poly(L-lactic acid)/chitosan blends with nano-hydroxyapatite[127]	Thermally induced phase separation method/M_w of 250,000 g/mol with ~90% DDA	• Enhanced compression modulus from 15.4 to 25.5 MPa, strength from 1.42 to 1.63 MPa • Improved rate of biodegradation, ALP activity and osteoconductivity	Rabbit marrow mesenchymal stem cells (MSCs)
Nano silica reinforced chitosan and alginate blend[128]	Freeze drying approach/low-molecular-weight and 75%–85% of DDA with 20–300 cPs viscosity	• Nano silica facilitated the adsorption of proteins and swelling ability of nanocomposite scaffold • Enhanced the apatite layer formation and no significant toxicity found even at higher doses of SiO_2 incorporation. • Nano silica encouraged differentiation ability (osteolineage) of the nanocomposite scaffolds as well	Osteoprogenitor cells. Cell viability increased up to ½-fold.
Nano-bioactive glass reinforced blends of chitosan-gelatin[129]	Freeze-drying approach/M_w of 100,000 to150,000 g/mol with ~85% DDA	• Reduced biodegradability as well as swelling ratio. • Enhanced cell attachment, proliferation and mineral deposition	MG-63 cells

(Continues)

TABLE 1 (Continued)

| Nanocomposites additives	Fabrication method and chitosan details (if available)	Features in comparison to pristine chitosan materials	Cell line and cytotoxicity in comparison to pristine chitosan materials evaluation (if available)
Nano-structured hydroxyapatite embedded in chitosan/cellulose blends[130]	Gradual electrostatic assembly/ Average M_w of 200,000–250,000 g/mol with 95.41% DDA	• No change was observed for % cell viability between control chitosan/cellulose blend membrane • Significant improvements of cell uptake and osteocalcin expression were noticed • Nanocomposites endorsed infiltration of bone tissues (in vivo) that led to better osteointegration, remodeling and rebuilding of bone defects	Primary osteoblast cells. Cell viability enhanced up to 12-fold after 11 days of culture for the nanocomposites scaffolds.
Nano hydroxyapatite reinforced blends of chitosan/poly(lactide-co-glycolide)[131]	Ultrasonic degassing/chitosan and poly(lactide-co-glycolide) weight ratio was 20:80	• Nanocomposite scaffolds showed amended mechanical stability, cell viability, adhesion, proliferation, and osteogenic differentiation capability	Human umbilical cord mesenchymal stem cells (hUCMSCs). Cell viability increased up to 4-fold after 11 days of culture.
Blends of gelatin and carboxy methyl chitosan reinforced with nano-hydroxyapatite[132]	Freeze-drying method/chemically modified chitosan had a medium-average M_w, 200-800 cP viscosity with 75–85% DDA	• Exhibited higher porosity, higher water retention capacity, as well as sustained enzymatic degradation rate, enhanced compressive strength • Biological activities were enhanced such as cell viability, proliferation, mineralization, new bone formation (in vivo). • Robust stem cell differentiation into osteogenic lineages like expression level of collagen type I, osteocalcin and Runx2	Human Wharton's jelly mesenchymal stem cells (hwjMSCs)
Doxycycline hyclate drug encapsulated hydroxyapatite nanoparticles embedded in blends of chitosan and hydroxyl propyl methyl cellulose[133]	Freeze-drying approach/average M_w of 188,000 g/mol with 80% DDA	• No burst release, sustained as well as enhanced cumulative drug release (95%) were found for the nanocomposite sponges • Slightly improved mechanical properties, and marginal improvement in biodegradation, cell viability, proliferation, drug release, alkaline phosphatase (ALP) for the nanocomposite sponges.	Mouse pre-osteoblasts, MC3T3-E1, cell viability enhanced by 25%
Injectable hydrogels made of blends of chitosan/collagen reinforced with hydroxyapatite nanoparticles[134]	Solution approach/average M_w of 250,000 g/mol with 95.6% DDA	• Incorporation hydroxyapatite nanoparticles enhanced % cell viability, new bone formation and collagen deposition	Allogeneic bone marrow derived mesenchymal stem cells
Injectable gel from blends of carboxymethyl–chitosan and gelatin reinforced with hydroxyapatite nanoparticles[135]	Solution approach, enzymatic crosslinking/carboxymethyl moieties modified chitosan has 70%–85% DDA	• Hydroxyapatite nanoparticles inclusion encouraged primary murine osteoblast proliferation, differentiation and osteoinductive characteristics	Primary murine osteoblast cells, cell viability enhanced up to 90%

T A B L E 1 (Continued)

Nanocomposites additives	Fabrication method and chitosan details (if available)	Features in comparison to pristine chitosan materials	Cell line and cytotoxicity in comparison to pristine chitosan materials evaluation (if available)
Chitosan coatings			
Hydroxyapatite on titanium surfaces[136]	Dip-coating approach	• Nanocomposites coating improved the hydrophilicity, % hemolysis, protein adsorption, biomineralization (apatite formation) and cell viability of titanium surfaces	MG 63 osteoblast cell lines
Hydroxyapatite nanohybrid on porous carbon fiber[137]	Dip-coating approach	• Nanohybrid coatings encouraged biomineralization, cell adhesion, spreading, and proliferation of porous carbon fiber felts.	Human bone marrow stromal cells, cell viability enhanced up to 4-fold
Silver and hydroxyapatite dual nanoparticles on TiO$_2$ substrate[138]	Anodization	• Nanocomposite coating showed prominent antimicrobial microbial efficacy against Gram-positive as well as Gram-negative bacterial strains • Slight improvement in cell viability	Mouse calvarial cells (MC3T3-E1), cell viability enhanced by 1-fold
Halloysite nanotube on titanium substrate[139]	Electrophoretic deposition/ Medium-average M$_w$ of 80,000 g/mol with 85% DDA	• Nanocomposites coatings enhanced the corrosion resistance, biomineralization, and hydrophilicity of titanium substrate	-

reinforced polycaprolactone–chitosan nanocomposites, and their tensile modulus was enhanced significantly compared to pristine polycaprolactone–chitosan samples prepared using a melt mixing approach. The mechanical properties such as tensile modulus and compression modulus of chitosan–gelatine based nanocomposite scaffolds were improved by 2-fold upon reinforcement with dual filler nanohydroxyapatite- nanoclay (montmorillonite).[141] Sun et al.[143] investigated the mechanical properties like tensile modulus and indentation hardness of chitosan/nanodiamond nanocomposites. The tensile modulus and indentation hardness of chitosan nanocomposites was enhanced by 343% and 127%, respectively upon 5 wt% nanodiamond filler loading. Comparative studies of the mechanical properties of porous chitosan nanocomposites scaffolds with various nanoparticles such as hydroxyapaptite, nano-zirconia, nano-calcium zirconate was carried out by Gaihr et al.[144] Among all, nano-calcium zirconate reinforced chitosan nanocomposites scaffold registered best mechanical strength like 5-fold improvement in compression modulus and 2.5 fold improvement in young's modulus. Caridade et al.[145] investigated the dynamic mechanical properties of bioactive glass nanoparticles reinforced chitosan nanocomposite membranes after

simulated body fluid immersion. Biomineralization and dynamic mechanical strengths like storage modulus (E′) and Tan δ were enhanced marginally for the chitosan nanocomposite membranes upon incorporation of bioactive glass nanoparticles.

Jiang et al.[130] fabricated spiral-cylindrical shaped nanocomposite scaffolds based on nano-hydroxyapatite incorporated into blends of chitosan and cellulose for bone regeneration applications. An in vitro MTT [3-(4,5-dimethylthiazol-2-yl)-2,5-diphenyltetrazolium bromide] assay suggested that there was no change concerning cell proliferation between the control sample and nanocomposites after 5 days of culturing. However, there was an increased cellular uptake and osteocalcin expression upon incorporation of 60-wt% of nano-hydroxyapatite filler into the blends. In vivo experiments with New Zealand white rabbits showed prominent improved osseointegration, complete infiltration of bone tissues, and NB formation in presence of the nanocomposite scaffolds compared to the control group. These features may facilitate the remodeling and rebuilding of bone defects rapidly. Figure 4 shows the key findings presented by X-ray photographs, 3D micro-CT results, and H&E stained histological tissue sections of
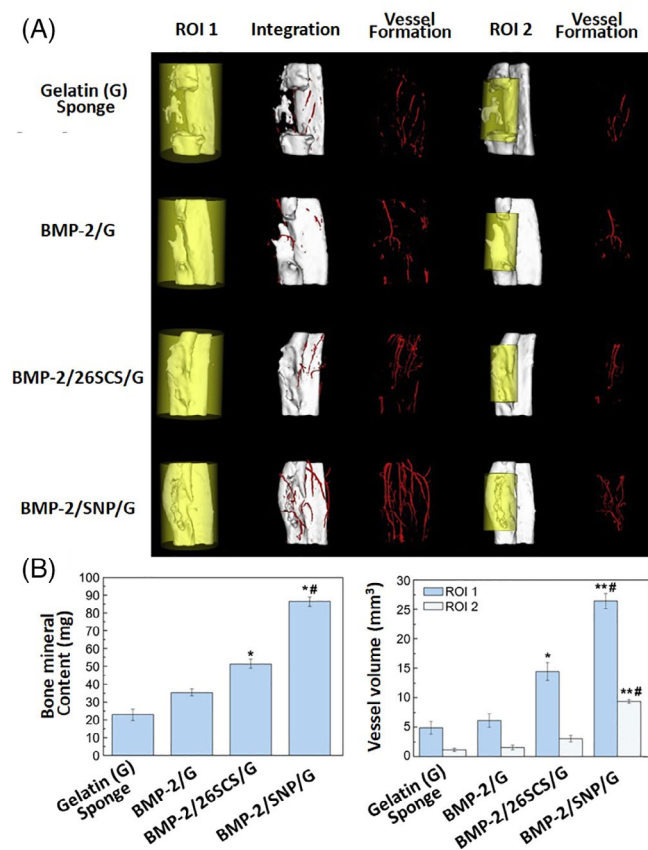
FIGURE 2 (A) Three dimensional micro-computed tomographic (μCT) images of various 2-*N*,6-*O*-sulfated chitosan-based nanocomposite sponges placed in two different regions of interest (ROI) in rabbits analyzed 4 weeks after implantation in comparison to a gelatin sponge. This images show the integration of new bone and vessel formation. ROI 1 reflects a cylindrical portion (30 mm height and 20 mm diameter) involving the radius and adjoining ulna with the defect site at the center and ROI 2 a cylindrical portion (18 mm in height) involving only the radius with the defect site at the center, (B) Quantitative determination of bone mineral content and blood vessel volume from μCT showing high numbers for the nanocomposite sample compared to that of others including the gelatin sponge. Gelatin sponge (G), bone morphogenetic Protein-2 (BMP-2), 2-*N*,6-*O*-sulfated chitosan 26SCS), and 2-*N*,6-*O*-sulfated chitosan nanoparticle (SNP) (Reproduced with permission from Cao et al.[140])

the control groups as well as the nanocomposite scaffolds. These combined results confirmed that the fabricated substrate is a suitable candidate for bone tissue-regeneration.

## 2.2 | Chitosan nanocomposites as wound dressings

In general, discontinuity in the skin occuring because of external laceration (accident) is called a wound. The

wound is classified in two major categories depending on healing rates. An acute wound heals faster, and a chronic wound takes more time to heal due to bacterial burden and larger discontinuity as two out of several factors. Wound healing has four stages namely hemostasis, inflammation, cell proliferation, and remodeling. Wound regeneration is a dynamic process comprising the secured action of inflammation, vascular as well as connective tissue production. Many biomaterials have been tested as wound dressings for acute and chronic wounds. The rate of healing varies depending upon the characteristics of the used biomaterials. Biomaterials should protect the wound from subordinate infections, absorb the wound fluids, support the tissue mechanically, avoid wound dehydration, and support cell differentiation. Chitosan-based nanocomposite substrates have received quite some attention due to various salient features such as excellent microbial rejection, O_2 permeability, photothermal effects, stimuli-responsiveness, and easy handling. It is able to process chitosan nanocomposites into thin-films, hydrogels, and fiber-meshes. The properties and characteristics of chitosan nanocomposites are better when the amount of nanoparticles is increased. Various nanoparticles including silver, iron, copper, zinc hydroxyapatite have been used as fillers for wound dressing applications. The various morphologies of chitosan nanocomposites and their key properties in context of wound dressing applications are summarized in Table 2.

Nirmal et al.[159] fabricated injectable nanostructured chitosan hydrogels with incorporated tigecycline and platelet-rich plasma for the treatment of infected wounds. Flow behavior as well as macroscopic observation of gel formation at various time points is shown in Figure 5. The rheological characteristics of the hybrid nanogels (tg-ChNPs-ChPRP) such as shear thinning improved the injectability. In an in vitro wound closure study using L929 cell migration best results were obtained in the presence of tg-ChNPs-ChPRP gels concerning antibacterial behavior, cell compatibility, hemocompatibility, drug release, and blood clotting characteristics. In vitro scratch wound closure studies are displayed in Figure 6 for a better understanding of the wound regeneration characteristics of the developed chitosan nanocomposites.

2.3 | Chitosan nanocomposites for drug delivery

Chitosan nanocomposites are often used in drug delivery applications to treat various diseases including cancer or osteoarthritis.[161] Drug embedded nanocomposites exhibit multifunctional properties such as excellent pharmacokinetics by delivering drugs at the desired site or tumor.
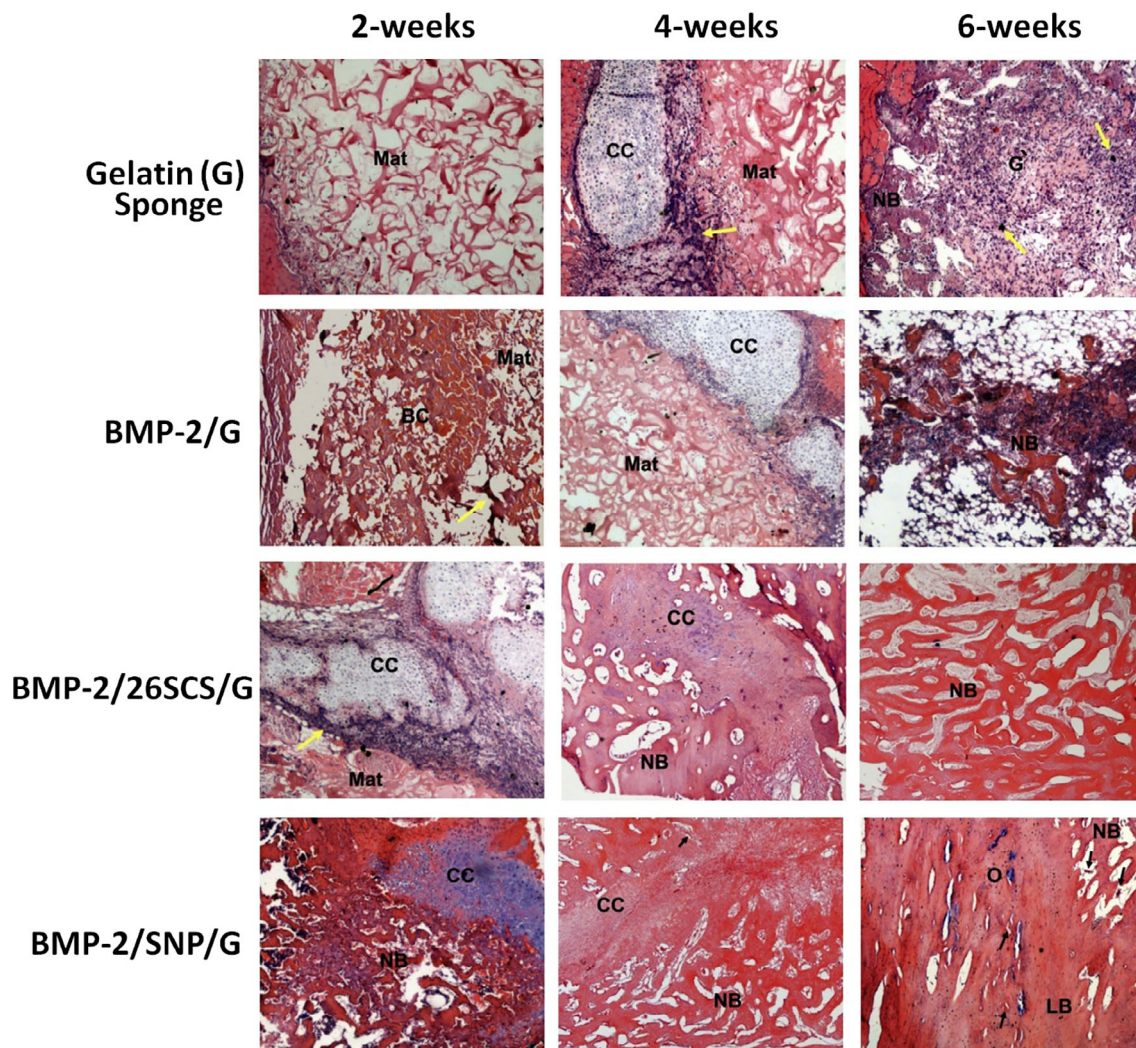
FIGURE 3 Hematoxylin and eosin (H&E)-stained sections of various 2-*N*,6-*O*-sulfated chitosan-based nanocomposite sponges placed in rabbits analyzed 2, 4, and 6 weeks after implantation compared to that of others including a gelatin sponge. The nanocomposite sponges show large amount of new bone, chondrocytes, macrophages and improved vasculogenesis. The following abbreviations are used Mat: implanted material; NB: new bone; BC: blood cell; G′: granulation tissue; CC: chondrocytes; LB: lamellar bone; yellow arrow: macrophages; black arrow: vasculogenesis, O: osteon) (Reproduced with permission from Cao et al.[140])

Stimuli-responsiveness helps to fine-tune drug release rates and avoids burst drug release. Drugs can be embedded efficiently in chitosan-based materials.[1] Chemical modifications of chitosan are one option to vary the amorphous nature of the materials with impact on drug loading efficiency and release characteristics.[7,17,28] Literature shows that there are many nanoparticles including reduced graphene oxide,[162] nanoclays,[163] gold nanoparticles,[164] mesoporous zeolites,[165] layered double hydroxide,[166] hydroxyapatite,[167] iron nanoparticle,[168] and SiO_2 nanoparticles[169] used for the fabrication of various types of chitosan-based drug delivery carrier. 2D layered nanosheets like MXenes (Ti_3C_2, Nb_2C) nanoclay, graphene or carbon nanotubes (CNT) display better release characteristics due to the generation of tortuous

pathway for clays yielding sustained release characteristics.[170] Furthermore, various researchers have also attempted to implement mesoporous silica and other nanoparticles including hydroxyapatite in chitosan matrices for fine tuning of drug loading efficiencies and release characteristics.[171–174] Their results suggest that pore size of the nanoparticles helped to encapsulate higher amounts of drugs (up to 90%) as well as to regulate the drug release at the desired site and time. Further, many nanoparticles like Ti_3C_2, Nb_2C, and carbon dots, CNT, graphene oxide and $GdPO_4$, and so forth have been used as photothermal agents for treating various tumors in NIR-I & NIR-II biowindows.[175,176] They showed excellent photothermal conversion efficiencies and rapid ablation of tumors. The photothermal-transformation efficiency
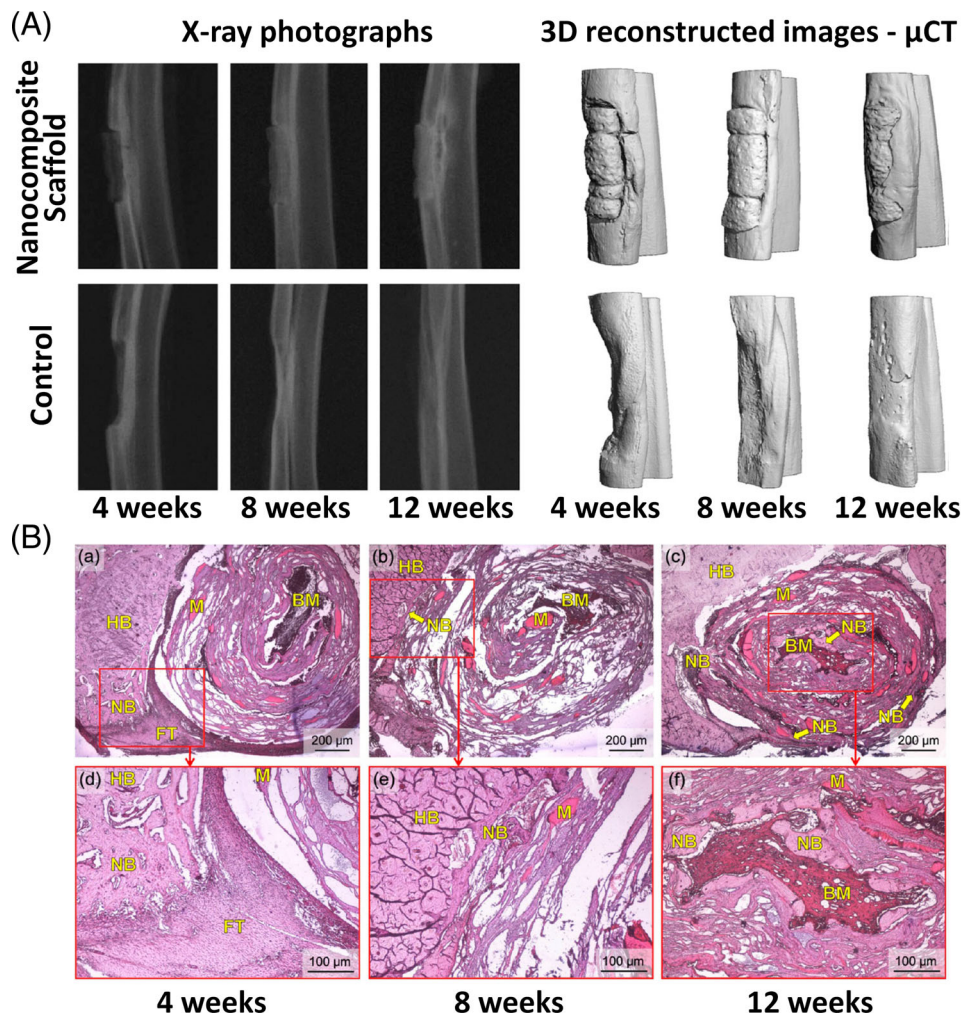
FIGURE 4 (A) X-ray radiographic photographs and three dimensional micro-computed tomographic (μCT) images of biomimetic spiral-cylindrical scaffolds based on blends of chitosan/cellulose placed in a concave defect in rabbits and analyzed at 4, 8, and 12 weeks after implantation. Comparison with a control scaffold showed new bone as well as callus tissue formation. (B) Hematoxylin and eosin (H&E)-stained sections of nanocomposite scaffolds implanted in rabbits analyzed at 4, 8 and 12 weeks to show the bone marrow and new bone formation (lower panel is the magnified portion of the red squares, which are marked in the upper panel). HB, NB, FT, BM, and M designates host bone, new bone, fibrotic tissue, bone marrow, and scaffold, respectively (Reproduced with permission from Jiang et al.[130])

of chitosan nanocomposite substrates helped to trigger drug release (%) at the target tissue.[176] A summary of drug delivery applications based on chitosan nanocomposites are compiled and summarized in Table 3.

Zhang et al.[188] developed chitosan hydrogels with incorporated magnetic nanoparticles and β-glycerophosphate for the sustained and long-lasting delivery of bacillus calmettee guérin for the treatment of bladder cancer. Figure 7 shows the preparation of the solution, its gel formation, drug encapsulation followed by how the sample behaves under a magnetic field. An intense and lasting $CD4^+$ lymphocytic infiltration was triggered in case of Fe_3O_4-BCG-CS/GP gels (group 4 samples). Figure 8 shows histological images of the various groups after CD4 staining. Rats in group 1 had 631 ± 78 CD4+ T cells and in group 3 had 508 ± 43.3 CD4+ T cells, whereas rats in group 2 had 2578 ± 268.7 CD4+ T cells and in group 4 had 3913 ± 466.7 CD4+ T cells showing multifocal lymphocytic infiltration. The results revealed that Fe_3O_4-BCG-CS/GP gels (group 4) had higher levels of $CD4^+$ T cells infiltrating the submucosa when compared to rats of the other groups. This result has been corroborated by the analysis of urinary cytokines as well and provides a first basis for antitumor treatment and induced high local immunity in the bladder.

Chandran and Sandhyarani[180] fabricated electric field responsive nanocomposite thin-films made of chitosan/gold nanoparticles and encapsulated 5-Fluorouracil (5-FU) by solution casting. The fabricated nanocomposites exhibited a higher drug release efficiency (63%) and sustained-release controlled by an external electric field (DC) in an electrolyte solution. The % human cervical cancer cell death was extremely high (above 90%) showing the efficiency of the anticancer effect.

Shah et al.,[148] fabricated chitosan/silver nanoparticle composite films with embedded moxifloxacin drugs by in-situ co-precipitation. The drug-encapsulated nanocomposite films exhibited excellent mechanical properties as well as antimicrobial efficacy against the various pathogens. They also exhibited a higher swelling ratio, as

TABLE 2 Chitosan nanocomposite substrates for wound dressing

Nanocomposites additives	Fabrication method and chitosan details (if available)	Features in comparison to pristine chitosan materials	Cell line and cytotoxicity in comparison to pristine chitosan materials evaluation (if available)
Silver nanoparticles embedded in blend of chitosan-silk fibroin, *Bombyx mori*[146]	Solution casting/95% DDA and chitosan-silk fibroin ratio was 1:2	• Enhanced moisture retention capability, tensile strength and antimicrobial characteristics • In vivo studies showed controlled release of silver nanoparticle detected in liver, spleen and kidney, accelerated wound healing, reformed dermis layer with enriched blood vessels, enhanced collagen fiber synthesis, reduced inflammatory responses	No in vitro evaluation, only in vivo assessment
In situ generated silver nanoparticles/various types of chitosan[147]	In situ approach/three types of chitosan with low M_w of 369,000 g/mol, medium M_w of 1,278,000 g/mol and high M_w of 2,520,000 g/mol with varied DDA of 86%, 89%, 85%, respectively	• Chitosan served as a reducing and stabilizing agents of metal oxide precursors • Nanocomposites showed pronounced antimicrobial activity against Gram- (+) as well as Gram- (−) bacteria strains and almost zero cytotoxicity	Mammalian somatic (HaCaT) and Tumoral (A549) cells, cell viability was above 80% for both cells.
Moxifloxacin drug encapsulated in silver nanoparticle reinforced chitosan and sericin (*Bombyx mori*) blend films[148]	Solution blending/low M_w with 85% DDA	• Nanocomposite films promoted controlled release of drug with higher loading/releasing efficiency. • Drug encapsulated nanocomposite films showed excellent antimicrobial activity and full thickness wound healing efficiency by observing the formation of fibrosis, collagen fiber bundles reorganization, neovascularization, and thick epidermal layer (in vivo results)	No in vitro examination, only in vivo assessments
Layer-by-layer (LBL) fabricated scaffolds made of Chitosan and pectin/organic rectorite (OREC) deposited on cellulose acetate electrospun[149]	Electrospinning techniques/chitosan derived from shrimp shells, which has average M_w of 200,000 g/mol with 92% DDA	• Nanocomposite scaffolds showed great zone of microbial inhibition enhanced the cell compatibility at lower concentration of nanofiller loading	Human epidermal (EP) cells, cell viability was enhanced up to 2-fold.
Silver nanoparticles-encapsulated into blends of silk fibroin and carboxy methyl chitosan sponges[150]	Freeze-drying method/carboxy methyl moieties modified chitosan	• Silver nanoparticle reinforced nanocomposite sponges showed improved water absorption (%), retention capability, and water vapor transmission rate along with antimicrobial characteristics.	-

TABLE 2 (Continued)

| Nanocomposites additives	Fabrication method and chitosan details (if available)	Features in comparison to pristine chitosan materials	Cell line and cytotoxicity in comparison to pristine chitosan materials evaluation (if available)
Spherical nano silver particles incorporated in chitosan/ hyaluronic acid (HA) blended sponges[151]	Freeze-drying method/average M_W of 100,000–150,000 g/mol with 85% DDA. Chitosan and HA blend ratio was 5:1	• Silver nanoparticle reinforcement improved antibiotic resistant bacteria, antibacterial activity, zero toxicity and robust cell proliferation of the nanocomposite sponges	Human dermal fibroblasts, cell viability were about 75%.
Nano chondroitin sulfate encapsulated in blends of chitosan-hyaluronan (HYA) ternary sponges[152]	Freeze-drying method/average M_w of 100,000–150,000 g/mol with 85% DDA. Chitosan-HYA blend ratio is 2:1	• Ternary nanocomposites showed enhanced % swelling and blood clotting ability along with excellent cell compatibility	Human dermal fibroblasts, cell viability were about 90%.
Sponge-like microporous chitosan reinforced with silver and zinc oxide nanorods[153]	Lyophilization process/average M_W of 179,000 g/mol with ≥95% DDA	• Nanocomposite sponges displayed 88% of porosity, higher swelling ratio, and enhanced blood-clotting capability too. • Significantly enhanced the antimicrobial activity (In vitro and in vivo), full-thickness wound healing, re-epithelialization and denser collagen deposition.	Cellosaurus cell line (L02), cell viability was 95%.
Bilayer sponges from chitosan embedded with silver nanoparticles and chitosan– Bletilla striata polysaccharide[154]	Combination of oxidation and freeze-drying approach/ chitosan derived from crab shells having average M_w of ~235,000 g/mol with 93.7% DDA	• Nanocomposite bilayer sponge showed higher water retention, adequate mechanical properties and robust cellular uptake as well as cell proliferation • In vivo results depicted that enhanced healing rate of cutaneous wound followed by better mature epidermization with less inflammatory cells	L929 murine fibroblast cell line, cell viability was above 90%.
Sponges-based on chitosan/ hyaluronic acid blend enriched with andrographolide lipid nanoparticles[155]	Freeze-drying method/average M_w of 100,000–150,000 g/mol with 85% DDA	• In vivo results presented better wound healing characteristics, reduced scar formation and improved vascularisation • Nanocomposite sponges also exhibited anti-inflammatory and antioxidant effect	Only in vivo assessment
Silver nanoparticles incorporated in chitosan-l-glutamic acid/hyaluronic acid blend sponges[156]	Freeze-drying approach/average M_w of 300,000 g/mol with ≥85% DDA	• Nanocomposite sponges possessed good mechanical requisite, optimum swelling ratio, and higher water retention %, significant inhibition for the bacterial growth	L929 cells, cell viability was above 90%

TABLE 2 (Continued)

Nanocomposites additives	Fabrication method and chitosan details (if available)	Features in comparison to pristine chitosan materials	Cell line and cytotoxicity in comparison to pristine chitosan materials evaluation (if available)
		• Nanocomposite sponges showed no cell cytotoxicity at low concentrations of silver nanoparticles incorporation.	
		• In vivo results proved that wound contraction ratio, average healing time, and complete recovery of epithelium were prominent for the nanocomposite sponges	
Nanocomposites sponges from VEGF loaded fibrin nanoparticles encapsulated in chitosan/hyaluronic acid[157]	Freezing and lyophilisation approach/average M_w of 100,000–150,000 g/mol with 85% DDA	• Nanocomposite sponges showed controlled as well as higher amount (60%) of VEGF release. • Also, an excellent cell compatibility and capillary like tube formation were perceived for the HUVECs cultured on VEGF loaded fibrin nanoparticles-based nanocomposite sponges.	Human dermal fibroblast (HDF) cells and human umbilical vein endothelial cells (HUVECs). Cell viability enhanced to 98% after 48 h of culture.
Nanocomposites sponges from silver nanoparticles embedded in catechol-conjugated chitosan[158]	Freeze-drying approach/catechol-conjugated chitosan had an average M_n of 30,000 g/mol with 80% DDA	• Nanocomposite sponges possessed significant antibacterial activity but diminished % cell viability	MC3 T3 cells, cell viability enhanced to above 90% after 72 h of culture at lower concentration of silver
Tigecycline nanoparticles incorporated in chitosan/platelet-rich plasma (PRP) hydrogels[159]	In situ technique/average M_W of 100,000–150,000 g/mol with 85% DDA	• Nanocomposite hydrogels exhibited excellent in vitro, ex vivo and in vivo antibacterial activity, improved wound healing efficiency and sustained antibiotic release characteristics	L929 cell lines, cell viability increased up to 2-fold after 72 h of culture.
Blends of *N,O*-carboxymethyl chitosan and oxidized alginate hydrogels reinforced with nano-curcumin[160]	Solution blending approach/carboxymethyl moieties modified chitosan	• Addition of nano-curcumin improved sustained drug releases characteristics, enhanced the re-epithelialization of epidermis and collagen deposition (in vivo) of the nanocomposite hydrogels	No in vitro examination, only in vivo was performed

well as prolonged drug release up to 36 h, improved biodegradability, and biocompatibility (in vivo) in comparison to control chitosan films. Likewise, other drugs such as diclofenac sodium, doxorubicin (DOX), and 5-amino salicylic acid have been encapsulated in chitosan thin-films for cancer therapies.

Pifithrin-α (PFTα) was encapsulated in MgAl based layered double hydroxide reinforced chitosan nanocomposites using freeze-drying.[166] The nanocomposites showed a sustained drug release profile with 95% cumulative release but the initial burst release could not be prevented. However, mineral deposition, cell viability, proliferation, and
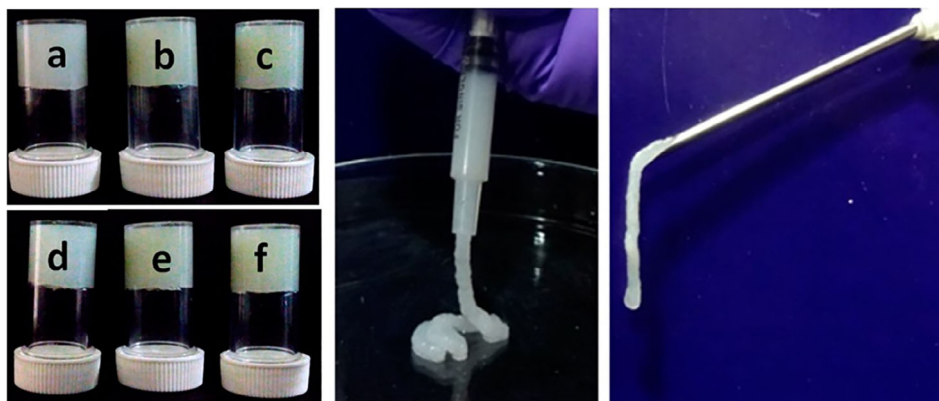
FIGURE 5 Inversion test for gel formation and improved rheological characteristics upon incorporation of tigecycline nanoparticles in chitosan-platelet-rich plasma (PRP) nanocomposite hydrogels (Reproduced with permission from Nimal et al.[159])
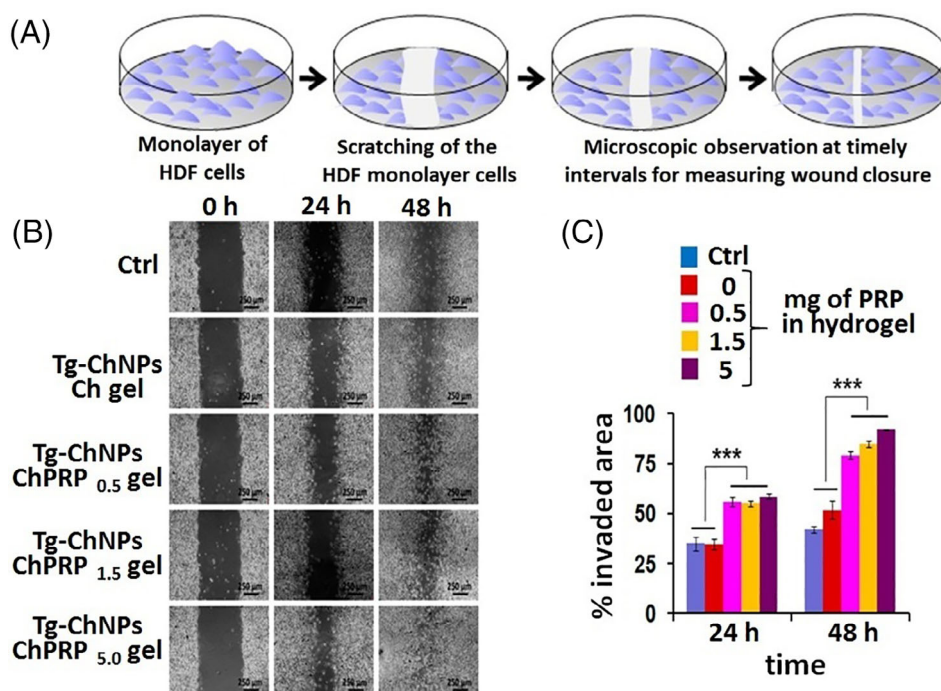
FIGURE 6 (A) Graphical representation of the in vitro wound closure experiment in a culture dish. (B) Images of L929 cell migration after 48 h of culturing in the presence of tigecycline nanoparticles reinforced chitosan−platelet-rich plasma (PRP) nanocomposite hydrogels with different concentrations of PRP compared to that of a control chitosan gel. (C) Area of % scratch wound closure of the nanocomposite hydrogel compared to that of a control chitosan gel (Reproduced with permission from Nimal et al.[159])

osteogenic differentiation were significantly enhanced in PFTα-embedded nanocomposite scaffolds. In-vitro human bone marrow mesenchymal stem cells (hBMSCs) proliferation was enhanced up to 3-fold and robust NB tissue formation was confirmed from in-vivo results.

2.4 | Chitosan nanocomposites for miscellaneous tissue engineering applications

Apart from the summarized applications in bone engineering, wound dressing, and for drug delivery applications, chitosan nanocomposites have been also other medical applications. They can be used as packaging films for storing drugs,[191] as coatings for metal electrodes, and medical kits, cardiac tissue engineering, and

electroactive tissue engineering.[192] Here, a selection is shown of miscellaneous tissue engineering applications of various chitosan nanocomposites which is summarized in Table 4. Various nanoparticles such as cetyltrimethylammonium bromide modified rectorite (REC) layered silicate,[185] iron,[85] silver, and manganese dioxides have been used to reinforce chitosan matrices for fabricating antimicrobial packaging films. The nanocomposite films showed excellent antimicrobial activity against gram-positive bacteria, gram-negative bacteria, and fungi with fast killing rates and more than 90% efficiency against several pathogens.

Jing et al.[206] fabricated an electroactive hydrogel made of chitosan/graphene oxide with self-healing capabilities as well as shape recovery for muscle tissue engineering applications. Polydopamine was tested as an oxidizing agent, which is a mussel-inspired agent for the

TABLE 3 Chitosan nanocomposite substrates for drug delivery

Nanocomposites additives	Fabrication method and chitosan details (if available)	Features in comparison to pristine chitosan materials	Cell line and cytotoxicity in comparison to pristine chitosan materials evaluation (if available)
Chitosan films			
5-Fluorouracil (5-FU) and curcumin (CU) co-encapsulated chitosan/reduced graphene oxide (rGO)[177]	Solution casting/low-molecular weight of 50,000–190,000 g/mol with 85% DDA	• Nanocomposite films showed excellent drug loading efficiency of 93% for 5-FU and 95% for CU and no burst release was observed • The dual drug encapsulated rGO nanocomposites enhanced anticancer activity of killed 80% of cancer cells as well compatible with fibroblasts	Human colon cancer cell lines (HT-29) and mouse embryonic fibroblast cells (NIH 3 T3). Cell viability was above 90% for fibroblasts whereas 80% cells were deed for HT-29
5-Fluorouracil (5-FU) encapsulated chitosan/silver nanoparticles/MWCNT[178]	Solution blending/low-molecular-weight with 85% DDA	• The drug loading efficiency was 96% for nanocomposites films and showed sustained release up to 72 h	MCF-7 cell line, % cell viability was above 85% at lower concentration loading of MWCNT
5-Fluorouracil (5-FU) encapsulated alginate-chitosan/montmorillonite (MMT) type clay[179]	Solution blending/medium-average-molecular weight with 85% DDA	• 5-FU drug encapsulated nanocomposite films with 30 wt% loading of MMT showed excellent performance in terms of loading and releasing efficiency • The burst release of drug was significantly higher for the nanocomposites films	-
5-Fluorouracil (5-FU) encapsulated in electric field responsive nanocomposites made of chitosan/gold nanoparticles[180]	Solution casting/average M_W of 270,000 g/mol with 85% DDA	• The drug release characteristics of nanocomposites were controlled by the external electric field (DC) in electrolyte solution • A higher drug release (63%) was obtained for the nanocomposites films at pH of 5.3 under external electric field. • The % cell death was extremely high for the drug encapsulated nanocomposites films, which show the efficiency of anticancer effect	Human cervical cancer cell lines SiHa, cell death was above 90%.
Diclofenac sodium embedded chitosan/MMT clay[181]	In situ solution casting/medium average M_W of 8,401,000 g/mol, viscosity of 200cPs with 80% DDA	• Drug encapsulated nanocomposite films showed many silent features such as controlled and prolonged drug release (up to 72 h and 54% release) with pH dependent manner • It also exhibited excellent antimicrobial activity and 50% cells were died	A549 cancer cells, cell death was up to 80%
Moxifloxacin embedded in chitosan/silver nanoparticles[182]	In situ approach followed by solution casting/low molecular weight with 85% DDA	• Drug encapsulated nanocomposite films exhibited excellent mechanical properties, antimicrobial efficacy against various pathogen	No in vitro examination, only in vivo assessments

(Continues)

TABLE 3 (Continued)

Nanocomposites additives	Fabrication method and chitosan details (if available)	Features in comparison to pristine chitosan materials	Cell line and cytotoxicity in comparison to pristine chitosan materials evaluation (if available)
		• It also exhibited higher swelling ratio, as well as prolonged drug release up to 36 h, improved biodegradability and biocompatibility (in vivo)	
Diclofenac encapsulated in chitosan/Na-beidellite clay[183]	Solution casting/98% DDA with a viscosity of 12 mPa s	• Drug embedded clay nanocomposites showed well intercalated morphology that enhanced the prolonged release of drug up to 8 h with cumulative drug release of 60% • Initial burst release of drug from nanocomposites films were controlled by upon increasing the addition of nanoclay as it induce more tortuous diffusion path	-
5-Amino salicylic acid (5-ASA) loaded modified chitosan/MMT[184]	Solution casting as well as melt mixing approach/chloro acetyl modified chitosan having average M_w of 400,000 g/mol with 70% DDA	• The prepared nanocomposite by both methods showed prolonged drug release up to 80 h and drug release efficacy was more than 90% with pH dependent. • The % cell death was more than 50%, which revealed the anticancer efficiency of drug encapsulated nanocomposite films	Human tumor cell lines (HCT15), cell death was above 50%
Doxorubicin (DOX) encapsulated quaternized chitosan/rectorite clay type[185]	Solution casting/2,3-epoxy propyl trimethyl ammonium chloride modified chitosan having average M_w of 200,000 g/mol with 92% DDA	• Drug loading efficiency and sustained release characteristics were enhanced upon incorporation of clay in chitosan films as it promotes more intercalated structure (morphology) • Cumulative drug release from nanocomposites films was significantly higher (85%) at basic condition (pH) and no burst release was observed	-
Doxorubicin embedded in pH responsive chitosan/ mesoporous zeolite[186]	Solution casting	• Nanocomposite films possessed drug loading efficiency of 95.8% with cumulative release of 88.6% under the tumor tissue pH of 5.5 • Drug release was only 49% at pH 7.4. and the cell compatibility was also pronounced for the drug encapsulated nanocomposites	MG63 and Human bone marrow derived mesenchymal stromal cells (hBMSCs), cell viability was above 85% for both cell lines

TABLE 3 (Continued)

Nanocomposites additives	Fabrication method and chitosan details (if available)	Features in comparison to pristine chitosan materials	Cell line and cytotoxicity in comparison to pristine chitosan materials evaluation (if available)
Chitosan scaffolds			
Pifithrin-α- (GS) encapsulated chitosan/hydroxyapatite[187]	Freeze-drying method	• GS-loaded hydroxyapatite microtube–CHS composites scaffolds showed excellent mechanical strength, high drug loading capability (97%), sustained drug release profile with reduced initial burst release • High antibacterial activity, cell adhesion, and biomineralization in comparison to hydroxyapatite nanorod reinforced scaffolds due to varied physical and morphological features of fillers	Rat bone marrow stromal cells (bMSCs), cell viability increased up to 2-fold
Pifithrin-α (PFTα) encapsulated in MgAl based layered double hydroxide[166]	Freeze-drying method	• Nanocomposites showed sustained drug release profile with 95% cumulative release but initial burst release was not able to control • Mineral deposition, cell viability, proliferation and osteogenic differentiation lineages such as COL1, ALP content RUNX2, OPN and OCN were significantly enhanced in PFTα-embedded nanocomposite scaffolds • In vivo results showed the new bone tissue formation	Human bone marrow mesenchymal stem cells (hBMSCs), cell proliferation was enhanced up to 3-fold
Magnetic hydrogels from iron nanoparticle[47]	Facile in situ hybridization method	• Fabricated magnetic hydrogels tenuously changed the drug release from passive release to pulsatile release under a low frequency alternating magnetic field An addition of iron nanoparticle enhanced the biocompatibility and mechanical strength including elastic modulus compared to that of pristine chitosan hydrogels	MG-63 cells, cell viability was 87%
Magnetic as well as thermos-sensitive hydrogels reinforced with β-glycerophosphate and Fe_3O_4 nanoparticles[188]	Solution blending approach/average M_W of 50,000 g/mol with 95% DDA	• Prolonged intravesical Bacillus Calmette–Guérin (BCG) residence time under magnetic field for the nanocomposite hydrogels • Improved antitumor effect as well as local immune activity was observed for the nanocomposite hydrogels upon incorporation of β-glycerophosphate and Fe_3O_4 nanoparticles	No in vitro examination, only in vivo was performed

(Continues)

TABLE 3 (Continued)

Nanocomposites additives	Fabrication method and chitosan details (if available)	Features in comparison to pristine chitosan materials	Cell line and cytotoxicity in comparison to pristine chitosan materials evaluation (if available)
Silica nanoparticles incorporated in thermo-sensitive hydrogels[189]	Solution approach/viscosity average M_W of 50,000–190,000 g/mol with 75%–85% DDA	• Increased humoral immunity and significantly induced CD^{4+} T cell proliferation upon incorporation of silica nanoparticles into chitosan hydrogels	No in vitro examination, only in vivo was performed
Thermo-responsive hydrogels made of hydroxyapatite and beta-glycerophosphate incorporated in thiolated chitosan-4-thio-butylamidine[190]	Solution approach/chitosan was chemically modified by 2-iminothiolane hydrochloride having a viscosity of 50–800 mPa, with 80%–95% DDA	• Rapid gelations, improved rheological behavior (shear thinning) as well biodegradability were observed for the nanocomposite hydrogels • Controlled protein release profile and no cytotoxicity were perceived upon incorporation of hydroxyapatite and beta-glycerophosphate in thiolated chitosan-4-thio-butylamidine hydrogels	Human bone-marrow mesenchymal stem cells (hMSCs). Cell viability increased up to 6-fold after 5 days of culture.

preparation of graphene oxide. The conductive graphene oxide significantly altered or improved cell viability as well as cell proliferation of human embryonic stem cell-derived fibroblasts and cardiomyocytes in the nanocomposites in comparison to pristine chitosan hydrogels. The impulsive beating rates of cardiomyocytes on the nanocomposites were two fold higher than the usual rate on tissue culture grade polystyrene (TCPS). Hence, conductive hydrogels can open new routes in modern muscle tissue engineering specifically in electrically active tissue like muscle, nervous or heart. They can help in regenerating the repaired tissues as well as integrate with the native tissue instantly.

Shao et al.[207] prepared chitosan sponges with incorporated silver sulfadiazine nanomaterials using a freeze-drying approach. The surface morphology of variously prepared sponges is shown in Figure 9. The cross-sectional view clearly shows the open porous three-dimensional network architecture of the sponge as well as the uniform pore sizes. The nanocomposites showed increased swelling ratios, porosity, and antimicrobial characteristics along with improved cell viability of human embryonic kidney 293 cells. However, there was an abrupt change in the cell morphology upon increasing the number of nanosilver particles above 5%. It is speculated that this is due to toxic effects.

Mitra et al.[198] fabricated copper-loaded acrylated quaternized chitosan/silica antibacterial coatings on poly(vinyl fluoride) films to impart antimicrobial activity. The nanocomposite coatings showed exceptional antimicrobial efficacies with 99% pathogen killing, and at the same time dermal fibroblast viability was enhanced up to 95%. The conductivity of chitosan nanocomposites has been effectively used for cardiac tissue engineering by incorporating novel conducting nanoparticles like CNT, graphene oxide, and carbon dots.

Pok et al.[200] fabricated nanocomposites by embedding single-walled CNT (SWCNT) in gelatin-chitosan blends. SWCNT showed some toxic effects upon increasing the dosage. At 175 ppm of SWCNT, the scaffolds showed only $47.7 \pm 6.9\%$ Neonatal Rat Ventricular Myocyte viability. This is a huge drawback concerning some applications. At 69 ppm or lower the scaffolds showed a better viability of 80%. Figure 10 shows the results of a live/dead cell assay on such scaffolds and differentiation capabilities indicated by the formation of sarcomeres (R-actinin = green) and gap junctions (connexin-43 = red). It inferred that SWCNT embedded gelatin/chitosan scaffolds performed as an electrical nanobridge between cardiomyocytes, which affected electrical coupling, synchronous beating, and cardiomyocyte function. Excitation conduction velocities of the nanocomposites were matching with that of the native myocardial tissue (22 ± 9 cm/s), which can regenerate cardiac defects including cardiac arrhythmias (in vivo).

FIGURE 7 Solution to gel transformation of various chitosan nanocomposite formulations: (A) control chitosan (CS)-β-glycerophosphate (GP) solution, (B) control chitosan-β-glycerophosphate gel, (C) Fe_3O_4-bacillus calmettee guérin (BCG)/CS/GP solution, (D) Fe_3O_4-BCG-CS/GP gel, (E) Fe_3O_4-BCG-CS/GP gels sink to the bottom of a beaker filled with saline buffer (F) the gel is attracted to an external magnet outside the beaker (Reproduced with permission from Zhang et al.[188])
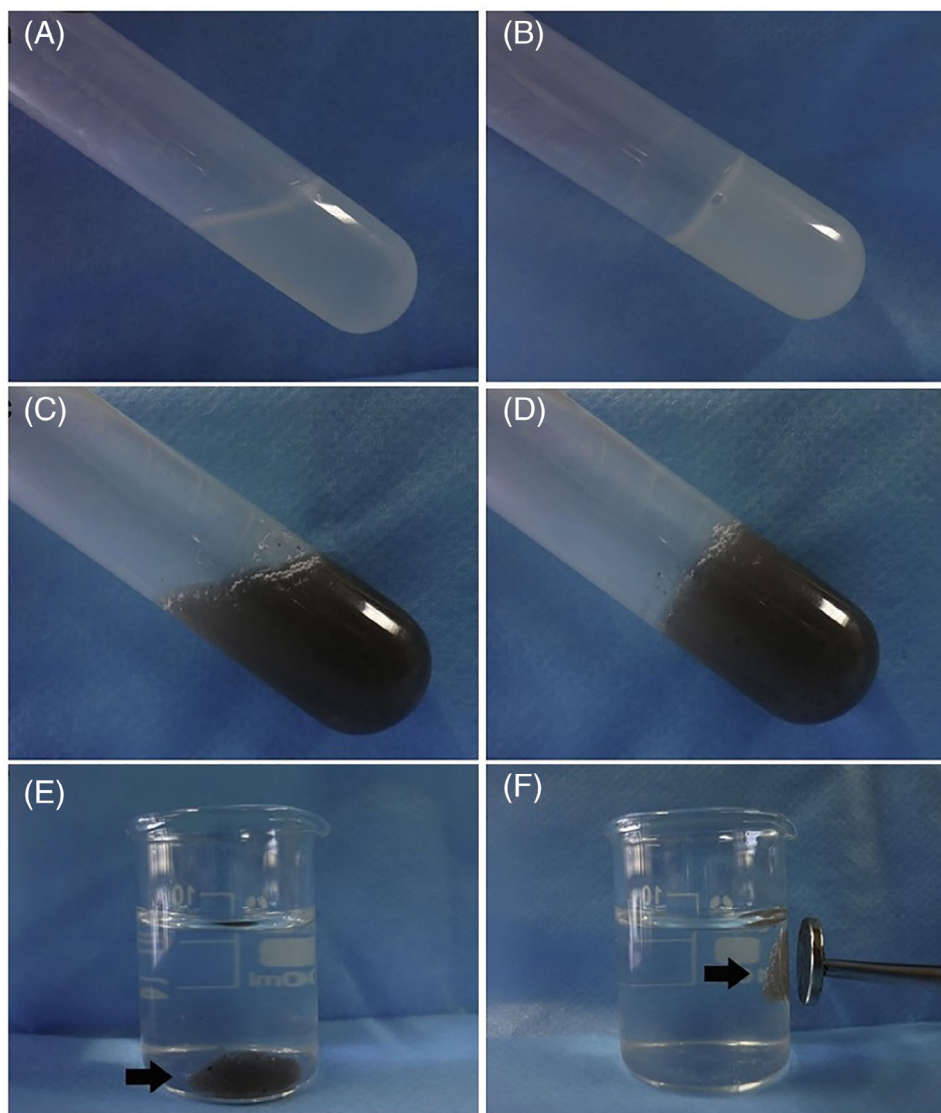
2.5 | Chitosan nanocomposites for biosensor applications

Biosensors are devices to convert physical, biological, and chemical signals of biological systems into an electrical one by identifying exact responses to target analytes.[208] A blood glucose biosensor is a classic example of a typical biosensor that uses the enzyme Glucose oxidase (GO_x). Electrochemical biosensors, as another example, specifically react with target moieties and generate an electrical signal related to specific analyte concentrations, pH, and temperature.[209] Biosensors play a key role in tissue engineering, and chitosan nanocomposites are also well used in these types of applications. In general, metal nanoparticles exhibit higher conductivity and electronic properties than conducting polymer, but the flexibility of polymers makes them unique for various applications. The addition of conducting nanoparticles to chitosan

materials enhances the electrical conductivity of the nanocomposites as well as stimuli-responsive characteristics, which could be used for sensing biological species.[210] For specifically enhancing the sensitivity toward biological moieties, biosensor surfaces have been modified using enzymes like cholesterol esterase (ChEt)[211] and cholesterol oxidase (ChOx)[212] to detect cholesterol content in blood or human serums. It has been shown that chitosan nanocomposites-based biosensors are more efficient, show a higher sensitivity, and are more durable in comparison to pristine chitosan.[210,212–218] There are many nanostructured inorganic materials such as cuprous oxide nanoparticles,[219] Fe_3O_4 nanoparticles,[218] $NiFe_2O_4$ nanoparticle,[217] Cerium oxide nanoparticle,[220] and TiO_2 nanoparticles[213] frequently used to enhance the electronic properties as well as the electrical conductivity of chitosan based materials in nanocomposites. Application examples are biosensors to detect cholesterol in human

(A)

(B)
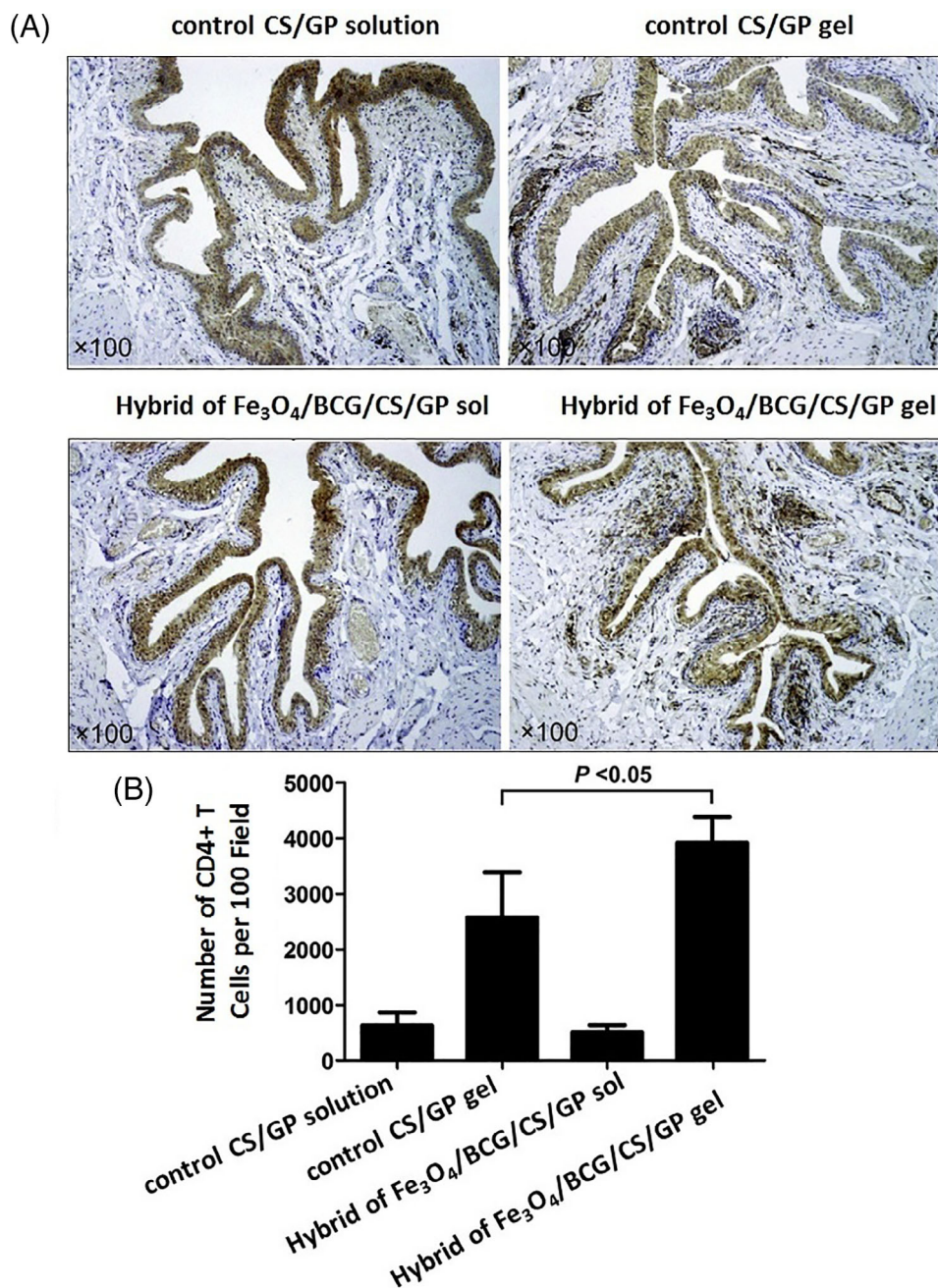
FIGURE 8 (A) Antibody (anti-CD4) stained section of various nanocomposite hydrogels placed inside of rat submucosa of a bladder analyzed 20 weeks after implantation. Immunohistochemistry photomicrographs showed that nanocomposite gels (Fe_3O_4-BCG-CS/GP) provoked more CD4+ activity compared to that of control chitosan gels with GP, (B) quantitative determination of CD4+ T cells per 100× magnification of corresponding micrographs. CS, GP, BCG denote chitosan, β-glycerophosphate and bacillus calmettee guérin, respectively (Reproduced with permission from Zhang et al.[188])

blood serum, glucose content in human serum and immunosensors for ochratoxin-A. Detailed features of various chitosan nanocomposites in biosensor applications are summarized in Table 5.

3 | CONCLUSIONS AND FUTURE PERSPECTIVES

Discussing their limitations is very important for improving material based explorations and new applications. Concerning chitosan nanocomposites, an increasing number of reports suggest that chitosan show great potential for biomedical applications. Studies portrayed in this review showcase that responses of tissues are remarkably different for chitosan nanocomposites in comparison to individual materials. Surface functionalization of nanoparticles and modifications of chitosan are important factors for directing cellular response, adhesion, proliferation, and differentiation. Moieties such as small biomolecules, peptides, proteins, and polymers are used to modulate the surface properties for enhanced biological responses facilitating better cell-substrate interaction, and improving mechanical properties of the substrate. Chitosan nanocomposites with tailored properties show favorable outcomes, such as faster

TABLE 4 Chitosan nanocomposite substrates for miscellaneous tissue engineering applications

Nanocomposites additives	Fabrication method and chitosan details (if available)	Features in comparison to pristine chitosan materials	Cell line and cytotoxicity in comparison to pristine chitosan materials evaluation (if available)	Application
Chitosan Films				
Cetyltrimethyl ammonium bromide modified rectorite (REC) layered silicate reinforced N-(2-hydroxyl) propyl-3-trimethyl ammonium chitosan chloride (HTCC)[193]	Solution casting/ chemically modified form of quaternized chitosan having weight average M_W of 210,000 g/mol	• The prepared clay nanocomposites showed well intercalated morphology and it exhibited excellent antimicrobial characteristics against Gram-positive bacteria, Gram-negative bacteria and Fungi as well • Also, nanocomposites displayed killing rate of more than 90% and cell walls has been destroyed rapidly for all the pathogen.	-	Antimicrobial packaging films
Manganese dioxide[194]	Solution casting/85% DDA	• The fabricated nanocomposite films performed as super adsorbent and inhibited bacterial growth about 50%	-	Antimicrobial packaging films
Graphene oxide embedded in blends of chitosan and poly (vinyl alcohol) matrix[195]	Solution casting/average low M_W of 144,000 g/mol with 90% DDA	• Graphene oxide contributed to enhance the microbial inhibition, mineral deposition and in vivo biodegradation without inflammatory response of the nanocomposite films	No in vitro evaluation, only in vivo assessment	Bone tissue engineering
Halloysite nanotube (HNT)[196]	Solution casting/viscosity-average M_W of 600,000 g/mol with 95% DDA	• HNT inclusion enhanced the surface roughness of the films, biocompatibility, static as well as dynamic mechanical properties of the nanocomposite films • Storage modulus increased by 193% upon incorporation of 7.5% HNT into chitosan matrix.	NIH3 T3 mouse fibroblasts	Muscle regeneration
Multiwalled carbon nanotubes (MWCNT)[197]	Solution casting/chitosan derived from crab shells	• Enhanced mechanical properties, cell metabolic activity as well as rate of cell proliferation	Endothelial cells and vascular myofibroblasts. Cell viability increased up to 2-fold for both cells.	Cardiovascular tissue engineering
Copper-loaded acrylated quaternized chitosan/silica antibacterial coatings on poly(vinyl fluoride) (PVF)[198]	Dip-coating approach/low average M_W having a viscosity of 0.02–0.3 kg/(m·s) with 75% DDA	• Copper-loaded nanocomposite coatings showed exceptional antimicrobial efficacies of about 99% bacteria were killed with high efficiency • Cell compatibility was also not affected by an inclusion of copper as well as silica	3 T3 mouse fibroblasts and adult human dermal fibroblasts, cell viability was enhanced up to 95% after 24 h of culture	Antimicrobial coatings for implants
Chitosan scaffolds				
Halloysite nanotubes scaffolds[199]	Combined solution-mixing and freeze-drying techniques/ chitosan had 95% DDA with a M_w of 600,000 g/mol	• Significant improvement in thermal stability, modulus and strength (compression more) was observed for the nanocomposite scaffolds • Biological characteristics such as cell uptake, adhesion and proliferation were enhanced significantly	Mouse fibroblasts NIH3T3-E1 cell line. Cell viability enhanced up to 2-fold after 4 days of culture.	Muscle tissue engineering

(Continues)

TABLE 4 (Continued)

Nanocomposites additives	Fabrication method and chitosan details (if available)	Features in comparison to pristine chitosan materials	Cell line and cytotoxicity in comparison to pristine chitosan materials evaluation (if available)	Application
Carbon nanotube embedded in blends of gelatin-chitosan[200]	Combined solution and sonochemistry approach	• Carbon nanotube embedded nanocomposit scaffold performed as an electrical nanobridges between cardiomyocytes, which enriched many features like electrical coupling, synchronous beating, and cardiomyocyte function • Excitation conduction velocities similar to that of the native myocardial tissue (22 ± 9 cm/s), which helped to regenerate cardiac defects including cardiac arrhythmias (in vivo)	Neonatal Rat Ventricular Myocyte (NRVM). Cell viability was above 80%.	Cardiac tissue engineering
Sponges-based on *Cuscuta reflexa* coated silver nanoparticles embedded in blends of chitosan and *Aloe vera* extract[201]	Freeze-drying approach/ chitosan derived from fungus of Cunninghamella elegans	• Nanocomposite sponges showed excellent antimicrobial activity against various pathogens • slightly decreased % cell viability	Human dermal fibroblast cell	Muscle tissue regeneration
Iron oxide decorated graphene oxide[202]	Solution approach/ average M_W of 193,400 g/mol with 77.7% DDA	• Significant improvements of antimicrobial activities against various gram-positive and gram-negative bacterial strains • Enhanced mechanical properties like tensile strength as well as modulus without comprising their biocompatibility	Mouse L929 fibroblastic cell line. Cell viability enhanced to above 87%	Antimicrobial biofilm
Alginate-*O*-carboxymethyl chitosan/nano fibrin[203]	Solution approach with ionic crosslinking/ chemical modified chitosan with alginate and carboxymethyl groups	• Nanocomposite hydrogels displayed improved mechanical properties • Cell adhesion, proliferation and differentiation into adipocytes was superior	Adipose derived stem cells (ADSCs). Cell viability increased up to 6-fold after 72 h of culture.	Adipose tissue engineering
Stimuli responsive hydrogels from chitosan/gold nanoparticles[204]	Solution approach/ medium molecular weight with 95% DDA	• Nanocomposite hydrogels possessed electrically conductive and showed active metabolism, migration and proliferation of MSCs • It also showed enhanced cardiomyogenic differentiation of MSCs	Mesenchymal stem cells (MSCs)	Cardiac tissue engineering
Chondroitin sulfate (CS) nanoparticles reinforced with chitosan grafted with poly(hydroxybutyrate-co-valerate) (CP) hydrogels[205]	Solution approach/ medium range M_W of 100,000–150,000 g/mol with 75%–85% DDA	• Nanocomposites hydrogels were mechanically stable, enhanced swelling characteristics and viscoelastic properties that closely mimic human nucleus pulposus • It also possessed excellent cell compatibility and supported chondrogenic differentiation of human mesenchymal stem cells	Adipose derived rat mesenchymal stem cells (ADMSCs). Cell viability increased up to 1-fold after 7 days of culture.	Nucleus pulposus tissue engineering

Control Chitosan $CS_{0.01\%}$ $CS_{0.02\%}$

$CS_{0.04\%}$ $CS_{0.08\%}$ $CS_{0.12\%}$
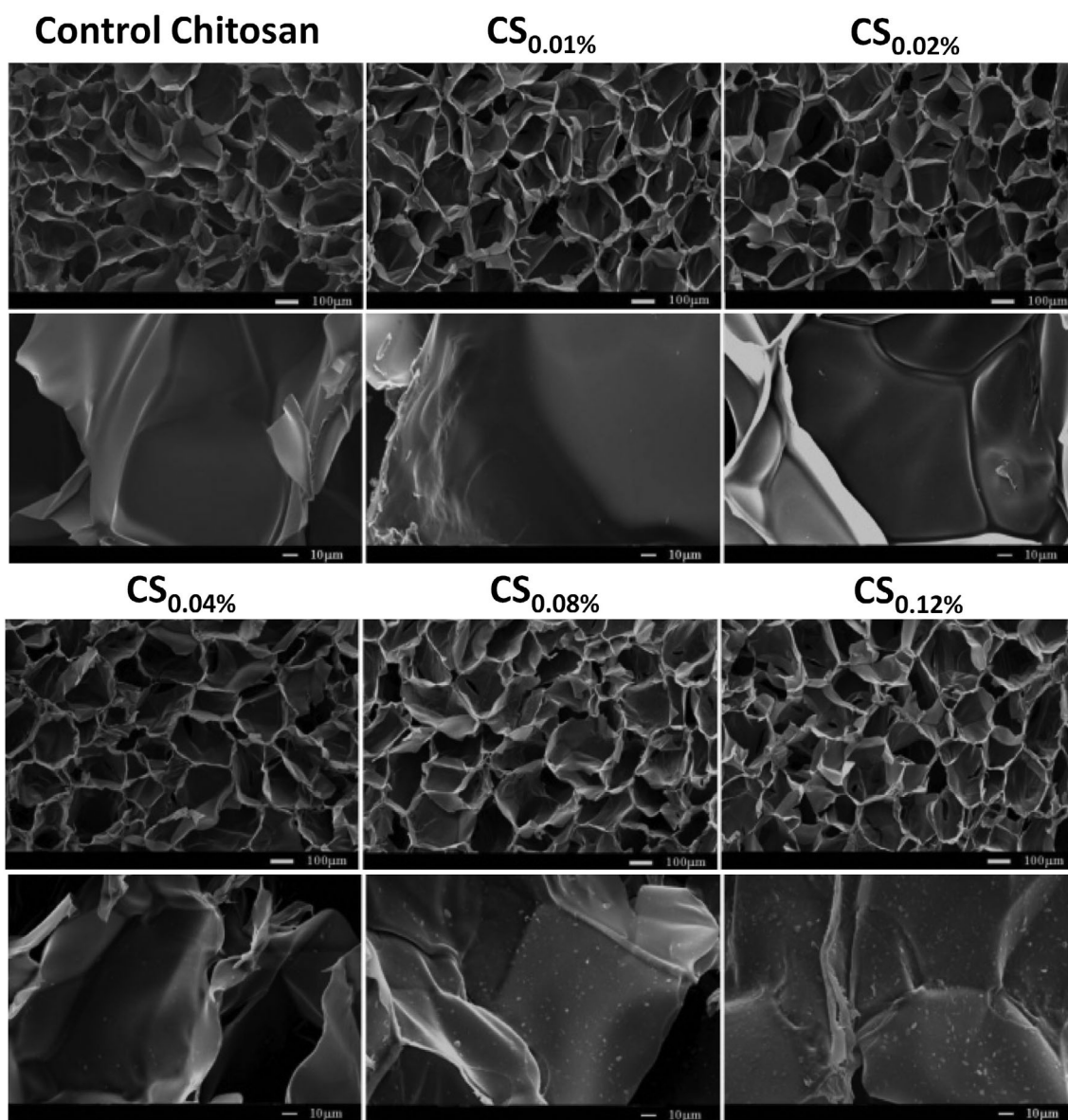
FIGURE 9 Cross sectional morphology of chitosan nanocomposite sponges reinforced with different amounts of silver sulfadiazine nanoparticles (Reproduced with permission from Shao et al.[207])

bone regeneration, targeted drug/cell delivery, better wound healing, enhanced angiogenesis, and osteogenesis. Nevertheless, comprehensive studies are necessary before clinical trials are initiated, since chitosan nanocomposites may elute over time and there is a need to investigate biodistribution in long-term animal trials. More specifically, nanoparticles released from the nanocomposites may be taken up by cells through endocytotic pathways, since nanoparticular graphene sheets have been shown to penetrate cells via clathrin-mediated endocytosis or via phagocytotic uptake. One already well-known minor drawback of chitosan is its inferior solubility in neutral solutions. Additionally, the molecular weight and DD severely affect the use of chitosan. Recently, one study

extensively investigated the biological characteristics of a library of chitosans with varying % DD, changes in the acetylation pattern and varying molecular weights.[223] It was identified that chitosan with more than 30,000 g/mol blocks glucosamine induced macrophage cytokines by lysosomal rupturing. Moreover, the concentration or quantity of nanoparticles used as fillers beyond a certain wt% decreases cell viability significantly, which is not a good basis for tissue engineering applications. Specifically, nanoparticles such as CNTs, silver sulfadiazine, and bioactive glass have shown toxic effects. Other nanoparticles did not improve any properties. Cell viability after 7 days of culture in presence of chitosan nanocomposites comprising halloysite nanotubes and
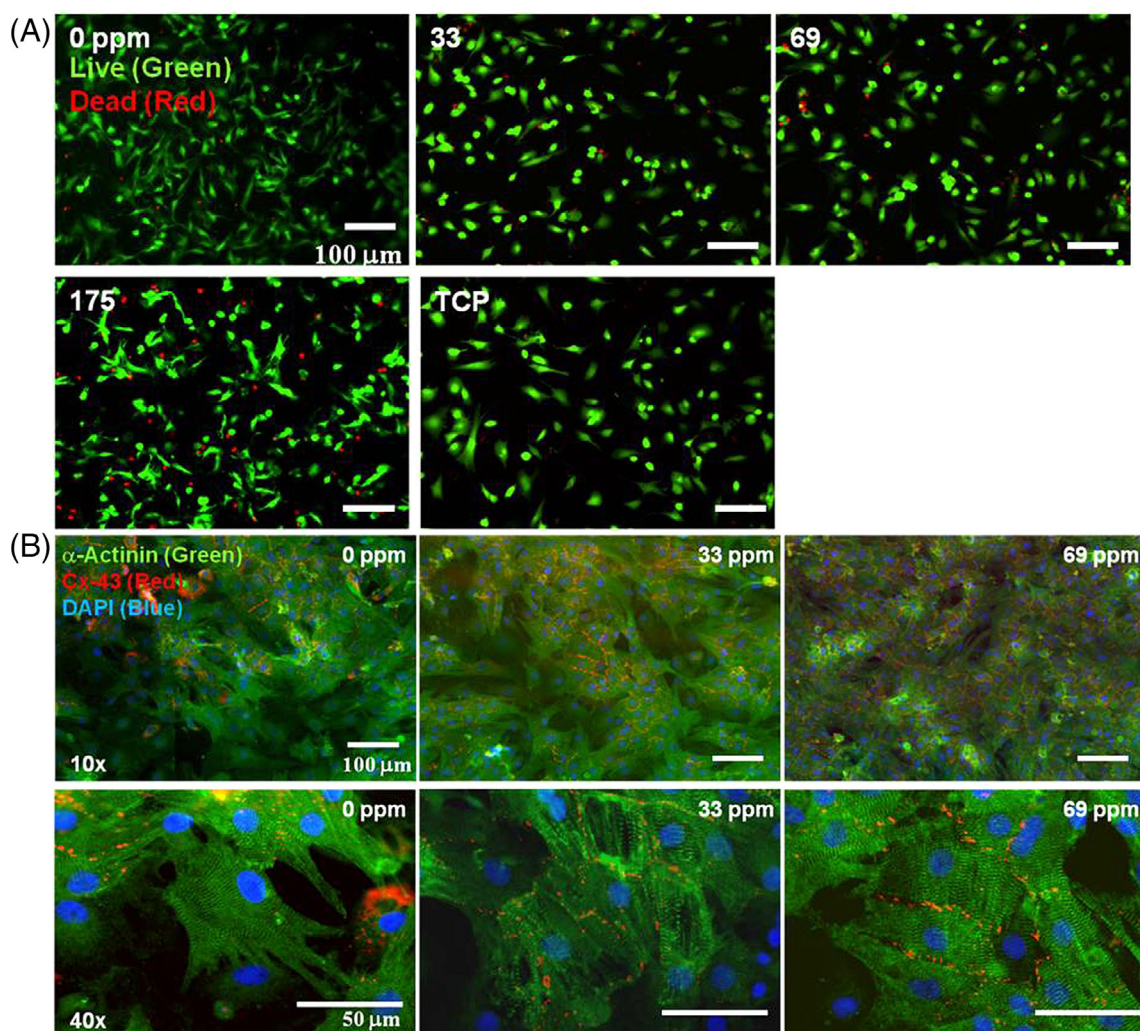
FIGURE 10 (A) Live/dead cell assay of neonatal rat ventricular myocytes (NRVM) cultured for 4 days on gelatin blended chitosan-based nanocomposite scaffolds with varying content (ppm) of single-walled carbon nanotubes (SWCNT) (B) immunostaining of sarcomeres (green for α-actinin) and gap junctions (red for connexin-43) displaying interconnected and integrated myocytes shows cell spreading upon increasing the amount of SWCNTs after 7 days of NRVM cell culture. (Adapted from Pok et al.[200])

TABLE 5 Chitosan nanocomposite films for biosensors applications

Nanocomposites additives	Fabrication method and chitosan details (if available)	Features in comparison to pristine chitosan materials	Application
Bioenzymes such as cholesterol esterase (ChEt) and cholesterol oxidase (ChOx)-functionalised cuprous oxide nanoparticle[221]	Solution casting/average low molecular weight with 85% DDA	• Functionalised nanoparticles reinforced nanocomposite films showed excellent biosensing characteristics to detect total cholesterol content in human blood serum with wide range (10–450 mg/dl), • High sensitivity of 0.895 μA/(mg/dl/cm^2), and ultra-fast response time (2 s).	Detect cholesterol in human blood serums
Fe$_3$O$_4$ nanoparticles embedded in chitosan/nafion blends[218]	Solution casting	• Showed excellent biosensing characteristics to detect total glucose content in human blood serum with high sensitivity (11.54 μA/cm^2/mM), and low detection limit (6 × 10^{-6} M).	Detect glucose content in human serums

TABLE 5 (Continued)

Nanocomposites additives	Fabrication method and chitosan details (if available)	Features in comparison to pristine chitosan materials	Application
Nanoparticles of $NiFe_2O_4$, CuO, and FeO; film surface was modified using cholesterol oxidase	Solution casting/low molecular weight with 80%–85% DDA	• Showed excellent biosensing characteristics to detect total cholesterol content in human blood serum with a low detection limit (313 mg/L), best linearity (50–5000 mg/L) • It also has ultra-fast response time (10 s), high sensitivity (0.043 μA/[mg/Lcm^2]), and a shelf-life of 3 months.	Detect cholesterol in human blood serum
$NiFe_2O_4$ nanoparticles[215]	Solution dip casting on glassy carbon electrode (GCE)	• Showed excellent electrocatalytical response to the oxidation of glucose. It exhibited fast response of less than 4 s, high sensitivity of 45.6 μA/(mmol/L/cm^2), low detection limit of 1.0–8.0 mmol/L and long-term stability of up to 30 days	Amperometric glucose biosensor
chitosan–polypyrrole[214]	Solution dip casting on glassy carbon electrode (GCE)	• Showed excellent glucose sensing ability. It exhibited ultra-fast amperometric response time of less than 5 s, and broad range of detection limit from 5.00×10^{-4} to 1.47×10^{-1} M including low detection limit (1.55×10^{-5} M).	Glucose biosensor
Ceriumoxide nanoparticles; film surface was modified using cholesterol oxidase[216]	Solution dip casting on indium-tinoxide (ITO) coated glass plate/average M_W of 2,400,000 g/mol	• The nanocomposite thin films formed on ITO plate showed wide detection range of 10–400 mg/dl with a limit of 5 mg/dl • It also showed ultra-fast response time of less than 10 s, high sensitivity of 47 μA/mg/dl/cm^2 and regression coefficient of 0.994.	Detect cholesterol in human blood serum
TiO_2 nanoparticles; film surface was modified using Ochratoxin-A (*Aspergillus ochraceus*)[222]	Solution dip casting on indium-tinoxide (ITO) plate/average M_W of 2,400,000 g/mol	• The nanocomposite thin films formed on ITO plate showed detection response of up to 10 ng/ml, detection sensitivity of 7.5 mM	Immunosensor for ochratoxin-A detection

calcium phosphate resulted in the same cell viability (%) as in the control samples. However, despite various flaws of chitosan nanocomposite substrates, they hold a great potential for biomedical applications.

ORCID
Thomas Scheibel https://orcid.org/0000-0002-0457-2423

REFERENCES
[1] S. Pradhan, A. K. Brooks, V. K. Yadavalli, *Mater. Today Bio* **2020**, *7*, 100065.
[2] M. Sakai, T. Seki, Y. Takeoka, *Small* **2018**, *14*, e1800817.
[3] Q. Cheng, C. Huang, A. P. Tomsia, *Adv. Mater.* **2017**, *29*, 1703155.
[4] U. G. Wegst, H. Bai, E. Saiz, A. P. Tomsia, R. O. Ritchie, *Nat. Mater.* **2015**, *14*, 23.
[5] C. Ortiz, M. C. Boyce, *Science* **2008**, *319*, 1053.
[6] J. G. Hardy, T. R. Scheibel, *Prog. Polym. Sci.* **2010**, *35*, 1093.
[7] S. Dai, P. Ravi, K. C. Tam, *Soft Matter* **2008**, *4*, 435.
[8] R. A. Muzzarelli, J. Boudrant, D. Meyer, N. Manno, M. DeMarchis, M. G. Paoletti, *Carbohydr. Polym.* **2012**, *87*, 995.
[9] K. Tokuyasu, H. Ono, K. Hayashi, Y. Mori, *Carbohydr. Res.* **1999**, *322*, 26.

[10] R. A. G. Harmsen, B. B. Aam, J. Madhuprakash, A. G. Hamre, E. D. Goddard-Borger, S. G. Withers, V. G. H. Eijsink, M. Sorlie, *Biochemistry* **2020**, *59*, 4581.

[11] H. Liu, C. Y. Wang, C. Li, Y. G. Qin, Z. H. Wang, F. Yang, Z. H. Li, J. C. Wang, *RSC Adv.* **2018**, *8*, 7533.

[12] T. H. Kim, H. L. Jiang, D. Jere, I. K. Park, M. H. Cho, J. W. Nah, Y. J. Choi, T. Akaike, C. S. Cho, *Prog. Polym. Sci.* **2007**, *32*, 726.

[13] H. Sashiwa, N. Kawasaki, A. Nakayama, E. Muraki, N. Yamamoto, S. Aiba, *Biomacromolecules* **2002**, *3*, 1126.

[14] B. Klaykruayat, K. Siralertmukul, K. Srikulkit, *Carbohyd. Polym.* **2010**, *80*, 197.

[15] R. Jayakumar, N. Selvamurugan, S. V. Nair, S. Tokura, H. Tamura, *Int. J. Biol. Macromol.* **2008**, *43*, 221.

[16] S. K. Shukla, A. K. Mishra, O. A. Arotiba, B. B. Mamba, *Int. J. Biol. Macromol.* **2013**, *59*, 46.

[17] M. R. Kumar, R. A. Muzzarelli, C. Muzzarelli, H. Sashiwa, A. Domb, *Chem. Rev.* **2004**, *104*, 6017.

[18] T. Aigner, T. Scheibel, *ACS Appl. Mater. Interfaces* **2019**, *11*, 15290.

[19] J. Kumirska, M. X. Weinhold, J. Thöming, P. Stepnowski, *Polymer* **2011**, *3*, 1875.

[20] S. M. Upadrashta, P. R. Katikaneni, N. O. Nuessle, *Drug Dev. Ind. Pharm.* **1992**, *18*, 1701.

[21] D. Fong, M. B. Ariganello, J. Girard-Lauzière, C. D. Hoemann, *Acta Biomater.* **2015**, *12*, 183.

[22] Y. Wang, H. Gu, *Adv. Mater.* **2015**, *27*, 576.

[23] A. Polini, D. Pisignano, M. Parodi, R. Quarto, S. Scaglione, *PLoS One* **2011**, *6*, e26211.

[24] M. Lutolf, J. Hubbell, *Nat. Biotechnol.* **2005**, *23*, 47.

[25] X. Liu, J. Chen, C. Qu, G. Bo, L. Jiang, H. Zhao, J. Zhang, Y. Lin, Y. Hua, P. Yang, N. Huang, Z. Yang, *ACS Biomater. Sci. Eng.* **2018**, *4*, 1568.

[26] Z. S. Haidar, R. C. Hamdy, M. Tabrizian, *Biomaterials* **2008**, *29*, 1207.

[27] K. Pieklarz, M. Tylman, Z. Modrzejewska, *Mini-Rev. Med. Chem.* **2020**, *20*, 1619.

[28] F. Ahmed, F. M. Soliman, M. A. Adly, H. A. M. Soliman, M. El-Matbouli, M. Saleh, *Res. Vet. Sci.* **2019**, *126*, 68.

[29] K. Kalantari, A. M. Afifi, H. Jahangirian, T. J. Webster, *Carbohydr. Polym.* **2019**, *207*, 588.

[30] S. Dimassi, N. Tabary, F. Chai, N. Blanchemain, B. Martel, *Carbohydr. Polym.* **2018**, *202*, 382.

[31] A. Rafique, K. Mahmood Zia, M. Zuber, S. Tabasum, S. Rehman, *Int. J. Biol. Macromol.* **2016**, *87*, 141.

[32] A. Usman, K. M. Zia, M. Zuber, S. Tabasum, S. Rehman, F. Zia, *Int. J. Biol. Macromol.* **2016**, *86*, 630.

[33] J. H. Ryu, S. Hong, H. Lee, *Acta Biomater.* **2015**, *27*, 101.

[34] S. Kumar, B. Krishnakumar, A. Sobral, J. Koh, *Carbohydr. Polym.* **2019**, *205*, 559.

[35] N. Naseri, C. Algan, V. Jacobs, M. John, K. Oksman, A. P. Mathew, *Carbohydr. Polym.* **2014**, *109*, 7.

[36] M. Zagorska-Dziok, P. Kleczkowska, E. Oledzka, R. Figat, M. Sobczak, *Int. J. Mol. Sci.* **2021**, *22*, 3339.

[37] X. Qing, G. He, Z. Liu, Y. Yin, W. Cai, L. Fan, P. Fardim, *Carbohydr. Polym.* **2021**, *261*, 117875.

[38] H. Y. Jung, P. Le Thi, K. H. HwangBo, J. W. Bae, K. D. Park, *Carbohydr. Polym.* **2021**, *261*, 117810.

[39] M. Yin, S. Wan, X. Ren, C. C. Chu, *ACS Appl. Mater. Interfaces* **2021**, *13*, 14688.

[40] O. Qianqian, K. Songzhi, H. Yongmei, J. Xianghong, L. Sidong, L. Puwang, L. Hui, *Int. J. Biol. Macromol.* **2021**, *181*, 369.

[41] G. Michailidou, Z. Terzopoulou, A. Kehagia, A. Michopoulou, D. N. Bikiaris, *Mar. Drugs* **2021**, *19*, 36.

[42] K. Kumamoto, T. Maeda, S. Hayakawa, N. A. B. Mustapha, M. J. Wang, Y. Shirosaki, *Polymers (Basel)* **2021**, *13*, 1104.

[43] W. Daniyal, Y. W. Fen, S. Saleviter, N. Chanlek, H. Nakajima, J. Abdullah, N. A. Yusof, *Polymers (Basel)* **2021**, *13*, 478.

[44] J. Xu, C. Y. Fu, Y. L. Tsai, C. W. Wong, S. H. Hsu, *Polymers (Basel)* **2021**, *13*, 326.

[45] A. Giannakas, K. Grigoriadi, A. Leontiou, N. M. Barkoula, A. Ladavos, *Carbohydr. Polym.* **2014**, *108*, 103.

[46] C. Vasile, R. N. Darie, C. N. Cheaburu-Yilmaz, G.-M. Pricope, M. Bračič, D. Pamfil, G. E. Hitruc, D. Duraccio, *Composites, Part B* **2013**, *55*, 314.

[47] B. Li, D. Jia, Y. Zhou, Q. Hu, W. Cai, *J. Magn. Magn. Mater.* **2006**, *306*, 223.

[48] H. Y. C. Eulalio, M. Vieira, T. B. Fideles, H. Tomas, S. M. L. Silva, C. A. Peniche, M. V. L. Fook, *Materials* **2020**, *13*, 5005.

[49] K. Hedayatyanfard, S. Bagheri-Khoulenjani, A. Hashemi, S. A. Ziai, *Iran. J. Pharm. Res.* **2019**, *18*, 1156.

[50] A. Mazloom-Jalali, Z. Shariatinia, I. A. Tamai, S. R. Pakzad, J. Malakootikhah, *Int. J. Biol. Macromol.* **2020**, *153*, 421.

[51] P. Hissae Yassue-Cordeiro, C. H. Zandonai, B. Pereira Genesi, P. Santos Lopes, E. Sanchez-Lopez, M. L. Garcia, N. R. Camargo Fernandes-Machado, P. Severino, B. S. E.,. C. Ferreira da Silva, *Pharmaceutics* **2019**, *11*, 1187.

[52] M. T. Soe, T. Pongjanyakul, E. Limpongsa, N. Jaipakdee, *Carbohydr. Polym.* **2020**, *245*, 116556.

[53] G. K. Abilova, D. B. Kaldybekov, G. S. Irmukhametova, D. S. Kazybayeva, Z. A. Iskakbayeva, S. E. Kudaibergenov, V. V. Khutoryanskiy, *Materials* **2020**, *13*, 1709.

[54] I. Buzzacchera, M. Vorobii, N. Y. Kostina, A. de Los Santos Pereira, T. Riedel, M. Bruns, W. Ogieglo, M. Moller, C. J. Wilson, C. Rodriguez-Emmenegger, *Biomacromolecules* **2017**, *18*, 1983.

[55] M. A. Bonifacio, S. Cometa, M. Dicarlo, F. Baruzzi, S. de Candia, A. Gloria, M. M. Giangregorio, M. Mattioli-Belmonte, E. De Giglio, *Carbohydr. Polym.* **2017**, *166*, 348.

[56] F. Ordikhani, E. Tamjid, A. Simchi, *Mater. Sci. Eng., C* **2014**, *41*, 240.

[57] S. Demeyer, A. Athipornchai, P. Pabunrueang, T. Trakulsujaritchok, *Carbohydr. Polym.* **2021**, *261*, 117905.

[58] C. Huang, Y. Liu, J. Ding, Y. Dai, L. Le, L. Wang, E. Ding, J. Yang, *Cell Tissue Res.* **2021**. https://www.stembook.org/node/39609.

[59] Y.-S. Han, S.-H. Lee, K. H. Choi, I. Park, *J. Phys. Chem. Solids* **2010**, *71*, 464.

[60] L. He, H. Wang, G. Xia, J. Sun, R. Song, *Appl. Surf. Sci.* **2014**, *314*, 510.

[61] A. Shah, I. Hussain, G. Murtaza, *Int. J. Biol. Macromol.* **2018**, *116*, 520.

[62] Q. Li, J. Zhou, L. Zhang, *J. Polym. Sci. Part B: Polym. Phys.* **2009**, *47*, 1069.

[63] P. Kaewklin, U. Siripatrawan, A. Suwanagul, Y. S. Lee, *Int. J. Biol. Macromol.* **2018**, *112*, 523.

[64] M. Sukul, P. Sahariah, H. L. Lauzon, J. Borges, M. Masson, J. F. Mano, H. J. Haugen, J. E. Reseland, *Carbohydr. Polym.* **2021**, *254*, 117434.

[65] Y. He, W. Zhao, Z. Dong, Y. Ji, M. Li, Y. Hao, D. Zhang, C. Yuan, J. Deng, P. Zhao, Q. Zhou, *Int. J. Biol. Macromol.* **2021**, *167*, 182.

[66] M. Ossama, C. Lamie, M. Tarek, H. A. Wagdy, D. A. Attia, M. M. Elmazar, *Drug Delivery* **2021**, *28*, 87.

[67] Y. Cheng, S. Lu, Z. Hu, B. Zhang, S. Li, P. Hong, *Int. J. Biol. Macromol.* **2020**, *164*, 3953.

[68] Y. Wang, K. Wang, J. Lin, L. Xiao, X. Wang, *Int. J. Biol. Macromol.* **2020**, *165*, 2684.

[69] K. Kanimozhi, S. K. Basha, K. Kaviyarasu, V. SuganthaKumari, *J. Nanosci. Nanotechnol.* **2019**, *19*, 4447.

[70] W. Sujka, Z. Draczynski, B. Kolesinska, I. Latanska, Z. Jastrzebski, Z. Rybak, B. Zywicka, *Materials* **2019**, *12*, 970.

[71] D. Porrelli, M. Mardirossian, L. Musciacchio, M. Pacor, F. Berton, M. Crosera, G. Turco, *ACS Appl. Mater. Interfaces* **2021**, *13*, 17255.

[72] F. Davani, M. Alishahi, M. Sabzi, M. Khorram, A. Arastehfar, K. Zomorodian, *Mater. Sci. Eng., C* **2021**, *123*, 111975.

[73] X. Su, T. Wang, S. Guo, *Regener. Ther.* **2021**, *16*, 63.

[74] N. Sahai, M. Gogoi, R. P. Tewari, *Curr. Med. Imaging* **2020**. https://doi.org/10.2174/1573405616666201217112939.

[75] P. Kazimierczak, K. Palka, A. Przekora, *Biomolecules* **2019**, *9*, 434.

[76] T. M. Sampath Udeni Gunathilake, Y. C. Ching, C. H. Chuah, H. A. Illias, K. Y. Ching, R. Singh, L. Nai-Shang, *Int. J. Biol. Macromol.* **2018**, *118*, 1055.

[77] X. Liu, M. Hao, Z. Chen, T. Zhang, J. Huang, J. Dai, Z. Zhang, *Biomaterials* **2021**, *272*, 120771.

[78] L. Muthukrishnan, *Carbohydr. Polym.* **2021**, *260*, 117774.

[79] T. Marimuthu, P. Kumar, Y. E. Choonara, *Expert Opin. Ther. Pat.* **2021**, 1744-7674.

[80] C. Benwood, J. Chrenek, R. L. Kirsch, N. Z. Masri, H. Richards, K. Teetzen, S. M. Willerth, *Bioengineering* **2021**, *8*, 27.

[81] S. V. Murphy, A. Atala, *BioEssays* **2013**, *35*, 163.

[82] S. A. Hosgood, M. Hoff, M. L. Nicholson, *Transplant Int.: Off. J. Eur. Soc. Organ Transplant.* **2021**, *34*, 224.

[83] S. A. R. Coelho, J. C. Almeida, I. Unalan, R. Detsch, I. M. Miranda Salvado, A. R. Boccaccini, M. H. V. Fernandes, *ACS Biomater. Sci. Eng.* **2021**, *7*, 491.

[84] E. H. Backes, E. M. Fernandes, G. S. Diogo, C. F. Marques, T. H. Silva, L. C. Costa, F. R. Passador, R. L. Reis, L. A. Pessan, *Mater. Sci. Eng., C* **2021**, *122*, 111928.

[85] R. Borges, L. Mendonca-Ferreira, C. Rettori, I. S. O. Pereira, F. Baino, J. Marchi, *Mater. Sci. Eng., C* **2021**, *120*, 111692.

[86] V. Campana, G. Milano, E. Pagano, M. Barba, C. Cicione, G. Salonna, W. Lattanzi, G. Logroscino, *J. Mater. Sci.: Mater. Med.* **2014**, *25*, 2445.

[87] N. Shibuya, D. C. Jupiter, *Clin. Podiatric Med. Surg.* **2015**, *32*, 21.

[88] L. E. Miller, J. E. Block, *Orthop. Res.Rev.* **2011**, *3*, 31.

[89] Y. Chen, J. Yu, Q. Ke, Y. Gao, C. Zhang, Y. Guo, *Chem. Eng. J.* **2018**, *341*, 112.

[90] Y.-Q. Tang, Q.-Y. Wang, Q.-F. Ke, C.-Q. Zhang, J.-J. Guan, Y.-P. Guo, *Chem. Eng. J.* **2020**, *387*, 124166.

[91] H. Xu, Y.-W. Ge, J.-W. Lu, Q.-F. Ke, Z.-Q. Liu, Z.-A. Zhu, Y.-P. Guo, *Chem. Eng. J.* **2018**, *354*, 285.

[92] X. Wen, F. Yang, Q.-F. Ke, X.-T. Xie, Y.-P. Guo, *J. Mater. Chem. B* **2017**, *5*, 7866.

[93] D. Kudasova, B. Mutaliyeva, K. Vlahovicek-Kahlina, S. Juric, M. Marijan, S. V. Khalus, A. V. Prosyanik, S. Segota, N. Spanic, M. Vincekovic, *Int. J. Mol. Sci.* **2021**, *22*, 2663.

[94] P.-P. Zhao, Y.-W. Ge, X.-L. Liu, Q.-F. Ke, J.-W. Zhang, Z.-A. Zhu, Y.-P. Guo, *Chem. Eng. J.* **2020**, *381*, 122694.

[95] S. Banerjee, B. Bagchi, S. Bhandary, A. Kool, N. A. Hoque, P. Biswas, K. Pal, P. Thakur, K. Das, P. Karmakar, S. Das, *Colloids Surf., B* **2018**, *171*, 300.

[96] A. P. Hurt, G. Getti, N. J. Coleman, *Int. J. Biol. Macromol.* **2014**, *64*, 11.

[97] Q. Yao, P. Nooeaid, R. Detsch, J. A. Roether, Y. Dong, O. M. Goudouri, D. W. Schubert, A. R. Boccaccini, *J. Biomed. Mater. Res., Part A* **2014**, *102*, 4510.

[98] J. Mota, N. Yu, S. G. Caridade, G. M. Luz, M. E. Gomes, R. L. Reis, J. A. Jansen, X. F. Walboomers, J. F. Mano, *Acta Biomater.* **2012**, *8*, 4173.

[99] A. Bhowmick, N. Pramanik, P. Jana, T. Mitra, A. Gnanamani, M. Das, P. P. Kundu, *Int. J. Biol. Macromol.* **2017**, *95*, 348.

[100] J.-w. Ai, W. Liao, Z.-L. Ren, *RSC Adv.* **2017**, *7*, 15971.

[101] P. Jongwattanapisan, N. Charoenphandhu, N. Krishnamra, J. Thongbunchoo, I.-M. Tang, R. Hoonsawat, S. M. Smith, W. Pon-On, *Mater. Sci. Eng., C* **2011**, *31*, 290.

[102] A. Bhowmick, N. Pramanik, T. Mitra, A. Gnanamani, M. Das, P. P. Kundu, *New J. Chem.* **2017**, *41*, 7524.

[103] J. Yang, A. Liu, Y. Han, Q. Li, J. Tian, C. Zhou, *J. Biomed. Mater. Res., Part A* **2014**, *102*, 1202.

[104] S. Saravanan, S. Nethala, S. Pattnaik, A. Tripathi, A. Moorthi, N. Selvamurugan, *Int. J. Biol. Macromol.* **2011**, *49*, 188.

[105] M. Shakir, S. Mirza, R. Jolly, A. Rauf, M. Owais, *New J. Chem.* **2018**, *42*, 363.

[106] M. Mazaheri, O. Akhavan, A. Simchi, *Appl. Surf. Sci.* **2014**, *301*, 456.

[107] J. Venkatesan, Z.-J. Qian, B. Ryu, N. A. Kumar, S.-K. Kim, *Carbohydr. Polym.* **2011**, *83*, 569.

[108] L. Chen, J. Hu, X. Shen, H. Tong, *J. Mater. Sci.: Mater. Med.* **2013**, *24*, 1843.

[109] S. Pattnaik, S. Nethala, A. Tripathi, S. Saravanan, A. Moorthi, N. Selvamurugan, *Int. J. Biol. Macromol.* **2011**, *49*, 1167.

[110] K. Jahan, G. Manickam, M. Tabrizian, M. Murshed, *Sci. Rep.* **2020**, *10*, 11603.

[111] H. Li, C.-R. Zhou, M.-Y. Zhu, J.-H. Tian, J.-H. Rong, *J. Biomater. Nanobiotechnol.* **2010**, *1*, 42.

[112] S. Elder, A. Gottipati, H. Zelenka, J. Bumgardner, *Open Orthop. J.* **2013**, *7*, 275.

[113] N. Siddiqui, K. Pramanik, E. Jabbari, *Mater. Sci. Eng., C* **2015**, *54*, 76.

[114] S. Shokri, B. Movahedi, M. Rafieinia, H. Salehi, *Appl. Surf. Sci.* **2015**, *357*, 1758.

[115] A. Shavandi, D. Bekhit Ael, M. A. Ali, Z. Sun, M. Gould, *Mater. Sci. Eng., C* **2015**, *56*, 481.

[116] J. Yang, T. Long, N. F. He, Y. P. Guo, Z. A. Zhu, Q. F. Ke, *J. Mater. Chem. B* **2014**, *2*, 6611.

[117] Y. He, Y. Dong, F. Cui, X. Chen, R. Lin, *PLoS One* **2015**, *10*, e0135366.

[118] P.-P. Zhao, H.-R. Hu, J.-Y. Liu, Q.-F. Ke, X.-Y. Peng, H. Ding, Y.-P. Guo, *Chem. Eng. J.* **2019**, *359*, 1120.

[119] F. Yang, J. Lu, Q. Ke, X. Peng, Y. Guo, X. Xie, *Sci. Rep.* **2018**, *8*, 7345.

[120] D. Zhou, C. Qi, Y. X. Chen, Y. J. Zhu, T. W. Sun, F. Chen, C. Q. Zhang, *Int. J. Nanomed.* **2017**, *12*, 2673.

[121] L. Cao, J. A. Werkmeister, J. Wang, V. Glattauer, K. M. McLean, C. Liu, *Biomaterials* **2014**, *35*, 2730.

[122] Y. Chen, F. Zhang, Q. Fu, Y. Liu, Z. Wang, N. Qi, *J. Biomater. Appl.* **2016**, *31*, 317.

[123] Y. Huang, X. Zhang, A. Wu, H. Xu, *RSC Adv.* **2016**, *6*, 33529.

[124] C. Sharma, A. K. Dinda, P. D. Potdar, C.-F. Chou, N. C. Mishra, *Mater. Sci. Eng., C* **2016**, *64*, 416.

[125] R. Jayakumar, R. Ramachandran, V. V. Divyarani, K. P. Chennazhi, H. Tamura, S. V. Nair, *Int. J. Biol. Macromol.* **2011**, *48*, 336.

[126] J. Liuyun, L. Yubao, Z. Li, L. Jianguo, *J. Mater. Sci.: Mater. Med.* **2008**, *19*, 981.

[127] X. Niu, Q. Feng, M. Wang, X. Guo, Q. Zheng, *J. Controlled Release* **2009**, *134*, 111.

[128] J. A. Sowjanya, J. Singh, T. Mohita, S. Sarvanan, A. Moorthi, N. Srinivasan, N. Selvamurugan, *Colloids Surf., B* **2013**, *109*, 294.

[129] M. Peter, N. Binulal, S. Soumya, S. Nair, T. Furuike, H. Tamura, R. Jayakumar, *Carbohydr. Polym.* **2010**, *79*, 284.

[130] H. Jiang, Y. Zuo, Q. Zou, H. Wang, J. Du, Y. Li, X. Yang, *ACS Appl. Mater. Interfaces* **2013**, *5*, 12036.

[131] F. Wang, X.-X. Su, Y.-C. Guo, A. Li, Y.-C. Zhang, H. Zhou, H. Qiao, L.-M. Guan, M. Zou, X.-Q. Si, *BioMed Res. Int.* **2015**, *2015*, 261938.

[132] S. Maji, T. Agarwal, J. Das, T. K. Maiti, *Carbohydr. Polym.* **2018**, *189*, 115.

[133] H. Iqbal, M. Ali, R. Zeeshan, Z. Mutahir, F. Iqbal, M. A. H. Nawaz, L. Shahzadi, A. A. Chaudhry, M. Yar, S. Luan, *Colloids Surf., B* **2017**, *160*, 553.

[134] Z. Huang, B. Yu, Q. Feng, S. Li, Y. Chen, L. Luo, *Carbohydr. Polym.* **2011**, *85*, 261.

[135] D. Mishra, B. Bhunia, I. Banerjee, P. Datta, S. Dhara, T. K. Maiti, *Mater. Sci. Eng., C* **2011**, *31*, 1295.

[136] B. Li, X. Xia, M. Guo, Y. Jiang, Y. Li, Z. Zhang, S. Liu, H. Li, C. Liang, H. Wang, *Sci. Rep.* **2019**, *9*, 14052.

[137] Y.-T. Liu, T. Long, S. Tang, J.-L. Sun, Z.-A. Zhu, Y.-P. Guo, *Mater. Lett.* **2014**, *128*, 31.

[138] W. Zhou, Y. Li, J. Yan, P. Xiong, Q. Li, Y. Cheng, Y. Zheng, *Sci. Rep.* **2018**, *8*, 13432.

[139] A. Molaei, A. Amadeh, M. Yari, M. Reza Afshar, *Mater. Sci. Eng., C* **2016**, *59*, 740.

[140] L. Cao, J. Wang, J. Hou, W. Xing, C. Liu, *Biomaterials* **2014**, *35*, 684.

[141] A. Olad, F. F. Azhar, *Ceram. Int.* **2014**, *40*, 10061.

[142] X. Xiao, R. Liu, Q. Huang, X. Ding, *J. Mater. Sci.: Mater. Med.* **2009**, *20*, 2375.

[143] Y. Sun, Q. Yang, H. Wang, *J. Funct. Biomater.* **2016**, *7*, 27.

[144] B. Gaihre, A. C. Jayasuriya, *Mater. Sci. Eng., C* **2018**, *91*, 330.

[145] S. G. Caridade, E. G. Merino, N. M. Alves, V. de Zea Bermudez, A. R. Boccaccini, J. F. Mano, *J. Mech. Behav. Biomed. Mater.* **2013**, *20*, 173.

[146] J. Liu, Z. Qian, Q. Shi, S. Yang, Q. Wang, B. Liu, J. Xu, X. Guo, H. Liu, *RSC Adv.* **2017**, *7*, 43909.

[147] A. Regiel-Futyra, M. Kus-Liśkiewicz, V. Sebastian, S. Irusta, M. Arruebo, A. Kyzioł, G. Stochel, *RSC Adv.* **2017**, *7*, 52398.

[148] A. Shah, M. A. Buabeid, E.-S. A. Arafa, I. Hussain, L. Li, G. Murtaza, *Int. J. Pharm.* **2019**, *564*, 22.

[149] W. Li, R. Xu, L. Zheng, J. Du, Y. Zhu, R. Huang, H. Deng, *Carbohydr. Polym.* **2012**, *90*, 1656.

[150] Z. Pei, Q. Sun, X. Sun, Y. Wang, P. Zhao, *Bio-Med. Mater. Eng.* **2015**, *26*, S111.

[151] B. Anisha, R. Biswas, K. Chennazhi, R. Jayakumar, *Int. J. Biol. Macromol.* **2013**, *62*, 310.

[152] B. Anisha, D. Sankar, A. Mohandas, K. Chennazhi, S. V. Nair, R. Jayakumar, *Carbohydr. Polym.* **2013**, *92*, 1470.

[153] Z. Lu, J. Gao, Q. He, J. Wu, D. Liang, H. Yang, R. Chen, *Carbohydr. Polym.* **2017**, *156*, 460.

[154] L. Ding, X. Shan, X. Zhao, H. Zha, X. Chen, J. Wang, C. Cai, X. Wang, G. Li, J. Hao, G. Yu, *Carbohydr. Polym.* **2017**, *157*, 1538.

[155] R. A.-B. Sanad, H. M. Abdel-Bar, *Carbohydr. Polym.* **2017**, *173*, 441.

[156] B. Lu, F. Lu, Y. Zou, J. Liu, B. Rong, Z. Li, F. Dai, D. Wu, G. Lan, *Carbohydr. Polym.* **2017**, *173*, 556.

[157] A. Mohandas, B. Anisha, K. Chennazhi, R. Jayakumar, *Colloids Surf., B* **2015**, *127*, 105.

[158] X. Huang, X. Bao, Z. Wang, Q. Hu, *RSC Adv.* **2017**, *7*, 34655.

[159] T. Nimal, G. Baranwal, M. Bavya, R. Biswas, R. Jayakumar, *ACS Appl. Mater. Interfaces* **2016**, *8*, 22074.

[160] X. Li, S. Chen, B. Zhang, M. Li, K. Diao, Z. Zhang, J. Li, Y. Xu, X. Wang, H. Chen, *Int. J. Pharm.* **2012**, *437*, 110.

[161] B. Sharma, S. Shekhar, P. Jain, R. Sharma, K. Chauhan, *Graphene Based Biopolymer Nanocomposites*, Singapore: Springer, **2021**, p. 135.

[162] M. S. Baktash, A. Zarrabi, E. Avazverdi, N. M. Reis, *J. Mol. Liq.* **2021**, *322*, 114515.

[163] V. Jauković, D. Krajišnik, A. Daković, A. Damjanović, J. Krstić, J. Stojanović, B. Čalija, *Mater. Sci. Eng., C* **2021**, *123*, 112029.

[164] H. Horo, S. Bhattacharyya, B. Mandal, L. M. Kundu, *Carbohydr. Polym.* **2021**, *258*, 117659.

[165] H. N. Abdelhamid, M. Dowaidar, Ü. Langel, *Microporous Mesoporous Mater.* **2020**, *302*, 110200.

[166] Y.-X. Chen, R. Zhu, Z.-l. Xu, Q.-F. Ke, C.-Q. Zhang, Y.-P. Guo, *J. Mater. Chem. B* **2017**, *5*, 2245.

[167] Y.-G. Zhang, Y.-J. Zhu, F. Chen, T.-W. Sun, *J. Mater. Chem. B* **2017**, *5*, 3898.

[168] F. Assa, H. Jafarizadeh-Malmiri, H. Ajamein, H. Vaghari, N. Anarjan, O. Ahmadi, A. Berenjian, *Crit. Rev. Biotechnol.* **2017**, *37*, 492.

[169] W. Liu, F. Wang, Y. Zhu, X. Li, X. Liu, J. Pang, W. Pan, *Molecules* **2018**, *23*, 3082.

[170] S. Murugesan, T. Scheibel, *Adv. Funct. Mater.* **2020**, *30*, 1908101.

[171] R. Kozakevych, Y. Bolbukh, V. Tertykh, *World J. Nano Sci. Eng.* **2013**, *3*, 69.

[172] A. Ahmed, J. Hearn, W. Abdelmagid, H. Zhang, *J. Mater. Chem.* **2012**, *22*, 25027.

[173] J. Zhang, G. Liu, Q. Wu, J. Zuo, Y. Qin, J. Wang, *J. Bionic Eng.* **2012**, *9*, 243.

[174] S. Pourshahrestani, E. Zeimaran, N. A. Kadri, N. Gargiulo, H. M. Jindal, S. V. Naveen, S. D. Sekaran, T. Kamarul, M. R. Towler, *ACS Appl. Mater. Interfaces* **2017**, *9*, 31381.

[175] Z. Su, D. Sun, L. Zhang, M. He, Y. Jiang, B. Millar, P. Douglas, D. Mariotti, P. Maguire, D. Sun, *Materials* **2021**, *14*, 2351.

[176] H. Wang, S. Mukherjee, J. Yi, P. Banerjee, Q. Chen, S. Zhou, *ACS Appl. Mater. Interfaces* **2017**, *9*, 18639.

[177] S. Dhanavel, T. Revathy, T. Sivaranjani, K. Sivakumar, P. Palani, V. Narayanan, A. Stephen, *Polym. Bull.* **2020**, *77*, 213.

[178] E. Nivethaa, S. Dhanavel, A. Rebekah, V. Narayanan, A. Stephen, *Mater. Sci. Eng., C* **2016**, *66*, 244.

[179] F. F. Azhar, A. Olad, *Appl. Clay Sci.* **2014**, *101*, 288.

[180] P. R. Chandran, N. Sandhyarani, *RSC Adv.* **2014**, *4*, 44922.

[181] D. Cheikh, F. García-Villén, H. Majdoub, C. Viseras, M. B. Zayani, *Int. J. Biol. Macromol.* **2019**, *126*, 44.

[182] A. Shah, M. A. Yameen, N. Fatima, G. Murtaza, *Int. J. Pharm.* **2019**, *561*, 19.

[183] D. Cheikh, F. García-Villén, H. Majdoub, M. B. Zayani, C. Viseras, *Appl. Clay Sci.* **2019**, *172*, 155.

[184] C. Aguzzi, P. Capra, C. Bonferoni, P. Cerezo, I. Salcedo, R. Sánchez, C. Caramella, C. Viseras, *Appl. Clay Sci.* **2010**, *50*, 106.

[185] J. Jin, H. Tu, J. Chen, G. Cheng, X. Shi, H. Deng, Z. Li, Y. Du, *Int. J. Biol. Macromol.* **2017**, *101*, 815.

[186] F. Yang, X. Wen, Q.-F. Ke, X.-T. Xie, Y.-P. Guo, *Mater. Sci. Eng., C* **2018**, *85*, 142.

[187] Y.-X. Chen, R. Zhu, Q.-F. Ke, Y.-S. Gao, C.-Q. Zhang, Y.-P. Guo, *Nanoscale* **2017**, *9*, 6765.

[188] D. Zhang, P. Sun, P. Li, A. Xue, X. Zhang, H. Zhang, X. Jin, *Biomaterials* **2013**, *34*, 10258.

[189] S. Gordon, E. Teichmann, K. Young, K. Finnie, T. Rades, S. Hook, *Eur. J. Pharm. Sci.* **2010**, *41*, 360.

[190] X. Liu, Y. Chen, Q. Huang, W. He, Q. Feng, B. Yu, *Carbohydr. Polym.* **2014**, *110*, 62.

[191] B. Ouattara, R. Simard, G. Piette, A. Begin, R. Holley, *J. Food Sci.* **2000**, *65*, 768.

[192] R. Khalili, P. Zarrintaj, S. H. Jafari, H. Vahabi, M. R. Saeb, *Int. J. Biol. Macromol.* **2020**, *154*, 18.

[193] X. Wang, Y. Du, J. Yang, X. Wang, X. Shi, Y. Hu, *Polymer* **2006**, *47*, 6738.

[194] Y. Anwar, *Int. J. Biol. Macromol.* **2018**, *111*, 1140.

[195] A. M. Pandele, M. Ionita, L. Crica, E. Vasile, H. Iovu, *Composites, Part B* **2017**, *126*, 81.

[196] D. Huang, Z. Zhang, Y. Zheng, Q. Quan, W. Wang, A. Wang, *Food Hydrocolloids* **2020**, *101*, 105471.

[197] A. Kroustalli, A. Zisimopoulou, S. Koch, L. Rongen, D. Deligianni, S. Diamantouros, G. Athanassiou, M. Kokozidou, D. Mavrilas, S. Jockenhoevel, *J. Mater. Sci.: Mater. Med.* **2013**, *24*, 2889.

[198] D. Mitra, M. Li, E.-T. Kang, K. G. Neoh, *ACS Appl. Mater. Interfaces* **2017**, *9*, 29515.

[199] M. Liu, C. Wu, Y. Jiao, S. Xiong, C. Zhou, *J. Mater. Chem. B* **2013**, *1*, 2078.

[200] S. Pok, F. Vitale, S. L. Eichmann, O. M. Benavides, M. Pasquali, J. G. Jacot, *ACS Nano* **2014**, *8*, 9822.

[201] D. E. L. Angulo, P. J. do Amaral Sobral, *Int. J. Biol. Macromol.* **2016**, *92*, 645.

[202] A. Konwar, S. Kalita, J. Kotoky, D. Chowdhury, *ACS Appl. Mater. Interfaces* **2016**, *8*, 20625.

[203] D. Jaikumar, K. Sajesh, S. Soumya, T. Nimal, K. Chennazhi, S. V. Nair, R. Jayakumar, *Int. J. Biol. Macromol.* **2015**, *74*, 318.

[204] P. Baei, S. Jalili-Firoozinezhad, S. Rajabi-Zeleti, M. Tafazzoli-Shadpour, H. Baharvand, N. Aghdami, *Mater. Sci. Eng., C* **2016**, *63*, 131.

[205] M. B. Nair, G. Baranwal, P. Vijayan, K. S. Keyan, R. Jayakumar, *Colloids Surf., B* **2015**, *136*, 84.

[206] X. Jing, H.-Y. Mi, B. N. Napiwocki, X.-F. Peng, L.-S. Turng, *Carbon* **2017**, *125*, 557.

[207] W. Shao, J. Wu, S. Wang, M. Huang, X. Liu, R. Zhang, *Carbohydr. Polym.* **2017**, *157*, 1963.

[208] N. J. Ronkainen, H. B. Halsall, W. R. Heineman, *Chem. Soc. Rev.* **2010**, *39*, 1747.

[209] J. Yao, M. Yang, Y. Duan, *Chem. Rev.* **2014**, *114*, 6130.

[210] C. Shan, H. Yang, D. Han, Q. Zhang, A. Ivaska, L. Niu, *Biosens. Bioelectron.* **2010**, *25*, 1070.

[211] G. Li, J. M. Liao, G. Q. Hu, N. Z. Ma, P. J. Wu, *Biosens. Bioelectron.* **2005**, *20*, 2140.

[212] S. Singh, P. R. Solanki, M. Pandey, B. Malhotra, *Sens. Actuators, B* **2006**, *115*, 534.

[213] H.-F. Cui, W.-W. Wu, M.-M. Li, X. Song, Y. Lv, T.-T. Zhang, *Biosens. Bioelectron.* **2018**, *99*, 223.

[214] Y. Fang, Y. Ni, G. Zhang, C. Mao, X. Huang, J. Shen, *Bioelectrochemistry* **2012**, *88*, 1.

[215] L. Luo, Q. Li, Y. Xu, Y. Ding, X. Wang, D. Deng, Y. Xu, *Sens. Actuators, B* **2010**, *145*, 293.

[216] B. D. Malhotra, A. Kaushik, *Thin Solid Films* **2009**, *518*, 614.

[217] J. Singh, M. Srivastava, P. Kalita, B. D. Malhotra, *Process Biochem.* **2012**, *47*, 2189.

[218] L. Yang, X. Ren, F. Tang, L. Zhang, *Biosens. Bioelectron.* **2009**, *25*, 889.

[219] S. Liu, M. Kang, F. Yan, D. Peng, Y. Yang, L. He, M. Wang, S. Fang, Z. Zhang, *Electrochim. Acta* **2015**, *160*, 64.

[220] A. Kaushik, P. R. Solanki, M. Pandey, S. Ahmad, B. D. Malhotra, *Appl. Phys. Lett.* **2009**, *95*, 173703.

[221] J. Singh, M. Srivastava, A. Roychoudhury, D. W. Lee, S. H. Lee, B. Malhotra, *J. Phys. Chem. B* **2013**, *117*, 141.

[222] R. Khan, M. Dhayal, *Electrochem. Commun.* **2008**, *10*, 492.

[223] D. Fong, P. Grégoire-Gélinas, A. P. Cheng, T. Mezheritsky, M. Lavertu, S. Sato, C. D. Hoemann, *Biomaterials* **2017**, *129*, 127.

AUTHOR BIOGRAPHIES

Selvakumar Murugesan received his bachelor's degree in polymer technology from Anna University, Chennai (India) in 2009 and master's degree in materials engineering from National Institute of Technology, Karnataka (India) in 2011. Then, he earned his doctoral degree from Indian Institute of Technology Kharagpur in the area of polymer hybrids for biomedical applications (2016). He was a postdoctoral student in Thomas Scheibel's group from 2018–2020 and worked on development of novel biomaterials based on recombinant spider silk proteins for tissue engineering applications. Currently, he is working as a junior professor at National Institute of Technology, Karnataka (India) in the department of

metallurgical and materials engineering. His research focuses on development of functional biomaterials for tissue engineering applications.

Thomas Scheibel has been full professor at the department of biomaterials at the Universität Bayreuth in Germany since 2007. He received both his diploma of biochemistry (1994) and a Dr. rer. Nat. (1998) from the Universität Regensburg in Germany. After his postdoctoral stay at the University of Chicago (1998–2001), he received his habilitation (2007) from the Technische Universität München in Germany. His research focuses on biotechnological production and processing of structural proteins, as well as their biomedical and technical application.